

The distributed biased min-consensus protocol revisited: pre-specified finite time control strategies and small-gain based analysis

Yuanqiu Mo, *Member, IEEE*, He Wang, *Member, IEEE*, Shuai Li, *Senior Member, IEEE*, and Wenwu Yu, *Senior Member, IEEE*

Abstract—Unlike the classical distributed consensus protocols that enable a group of agents to reach an agreement regarding a certain quantity of interest in a distributed fashion, the distributed biased min-consensus protocol (DBMC) has been proven to handle the advanced complexity of solving the shortest path problem. Such a protocol is commonly incorporated as the first step of a hierarchical architecture in real applications, such as robot path planning and the management of dispersed computing services. However, a major limitation of DBMC is the lack of results regarding its convergence within a user-assigned time frame. In this paper, we first propose two control strategies to ensure that the state error of DBMC decreases exactly to zero or a desired level within a finite time specified by the user. This paper further investigates the nominal DBMC itself. By leveraging small-gain based stability tools and embedding DBMC into a framework applicable to such tools, this paper also proves the global exponential input-to-state stability of DBMC, outperforming its current stability results. Simulations are provided to validate the efficacy of our theoretical results.

Index Terms—Consensus, Biased min-consensus, The shortest path problem, Pre-specified finite time control, Small-gain theorem

I. INTRODUCTION

The distributed consensus protocol, which aims to ensure that all agents reach an agreement in a distributed fashion, is one of the fundamental problems in the control field and has been extensively studied over the past decades [1]. Depending on the agreement value, consensus can be roughly divided into 3 categories: 1) average-consensus; 2) min-consensus; and 3) max-consensus, their merits can be observed in practical fields including formation control, clock synchronization, load balancing and so on [1]–[3]. Different from distributed consensus protocols which mainly serve as a means to mitigate state differences between agents, the distributed biased min-consensus protocol (DBMC) proposed in [4] has been proven to produce complex behaviors related to the shortest path problem [5],

which is a complicated combinatorial optimization problems studied in computer science and artificial intelligence. In particular, DBMC is capable of enabling each node in a graph to find the shortest path (in the sense that the sum of weights of its constituent edges is minimized) from its nearest source. Moreover, compared with the classical centralized shortest path algorithms, such as Dijkstra’s algorithm [6], Bellman-ford algorithm [5], A* algorithm [7], DBMC possesses better scalability and robustness. Specifically, 1) it is a distributed algorithm based on dynamic evolution; and 2) it achieves global stability as it has no requirement on the initial states, while the aforementioned classical methods all require the initial states to be infinity.

Given the above advantages of DBMC, stability of DBMC (especially the discretized version) has been well studied within the control community. [8]–[13] have demonstrated that the discrete-time DBMC and its variants converge within a finite number of iterations, providing different upper bounds for this number. Our prior work [12] also shows that the ultimate boundedness of the discrete-time DBMC under persistent perturbations on the edge weights, using a discrete-time Lyapunov-based approach. Owing to its finite time convergence, fruitful applications based on the discrete-time DBMC have explored. For instance, in [8], [11] the discrete-time DBMC is adopted to search the fastest charging station with the lowest overall objective and to discover the best supply candidate with minimum power loss in power and traffic networks, respectively. [10] utilizes the discrete-time DBMC to realize the optimal and safe path planning for unmanned surface vessels. In contrast to its discretized version, theoretical analyses of DBMC remain scarce. [4] proves the global asymptotic stability of DBMC via using LaSalle’s invariance principle. The regional exponential stability (requiring the initial states to be overestimates) of DBMC is further demonstrated in [14] by designing a non-smooth Lyapunov function. However, to the best of our knowledge, no existing work addresses the convergence of DBMC within a pre-specified time. This lack of research impedes the development of DBMC in real applications, where it is commonly incorporated as a core and initial part of the hierarchical architecture, necessitating its convergence in a prescribed time. For example, obtaining the optimal path for subsequent obstacles avoidance in robot path planning [10], or calculating the best route for the following management of dispersed computing services in content delivery networks [15]. Even though the discrete-

Yuanqiu Mo, He Wang and Wenwu Yu are with the Department of System Science, School of Mathematics, Southeast University, Nanjing 211189, China (email: yuanqiumo@seu.edu.cn, wanghe91@seu.edu.cn, wwyu@seu.edu.cn). Shuai Li is with the Faculty of Information Technology and Electrical Engineering, University of Oulu, Pentti Kaiteran katu 1, Oulu 90570, Finland, and also with Technology Research Center of Finland (VTT), Kaitovayla 1, Oulu 90570, Finland (email: shuai.li@oulu.fi). This work was supported by the National Science and Technology Major Project of China under Grant No. 2022ZD0120003, the National Natural Science Foundation of China under Grant No. 62303112, Grant No. 62203112 and Grant No. 62233004, and the Natural Science Foundation of Jiangsu Province under Grant No. BK20230826 and Grant No. BK20210216. (*Corresponding author: Wenwu Yu.*)

time DBMC can attain finite time convergence, the derived upper bounds on the finite time in existing literature are all defined by structural parameters of the graph, such as the number of nodes or the diameter [9], [10], [12], resulting in its inapplicability in situations where DBMC must complete within a given time. Moreover, the incompatibility between discrete-time DBMC and dynamical systems highlights the importance of developing a version of DBMC that guarantees convergence within a prescribed time.

Recently, pre-specified finite time (PT) control for nonlinear systems has garnered increasing attention. The salient feature of such control strategy is that it ensures the system stabilizes within a prescribed finite time, irrespective of initial conditions or any other design parameters [16]. This capability outperforms traditional finite time or fix time control strategies, whose settling times depend on either the initial states or a conservative estimate [17]. Furthermore, the PT stabilizing effect can be achieved by placing a novel but simple time-varying scaling function in the feedback loop [18], which allows it to be integrated into DBMC to guarantee convergence within a pre-specified time. However, infinite gain may occur at the presetting time instant while implementing PT control under noisy environment [17], [19], [20], limiting the practical usage of such method. To address this issue, practical pre-specified finite time (PPT) control has been proposed [21]. PPT control is a less ambitious version of PT control, ensuring that within the preset time, the state error converges to a neighborhood around the origin, with the magnitude adjustable by a user-defined parameter. Similar to PT control strategy, practical finite time stabilizing effect can be attained by employing a continuous time-varying function, such as a time base generator (TBG), as the feedback gain [22].

Motivated by the above PT, PPT control strategies and the urgent need for improving DBMC with user-defined convergence time, in this paper we provide three design strategies for DBMC suitable for various application scenarios. As for PPT stabilization, inspired by the convergence pattern of the shortest path where a node can determine its shortest path only after its parent node has done so, instead of using TBG directly, we repeatedly use the truncation of TBG to achieve the PPT stabilizing effect in an orderly manner, starting from the source node and extending to the entire network. For PT stabilization, technical issues arise as the feedback gain approaches infinity at the presetting time instant. By concatenating the time-varying scaling function with a constant and subtly designing an upper bound on the state error, we prove the continuity of the DBMC dynamics under PT control strategy, ensuring a continuous PT stable solution over the whole time interval. Turning back to the nominal DBMC with a constant feedback gain, we adopt a Lyapunov-based small-gain framework [23]–[25] to analyze its behaviors. A key technical challenge lies in modeling DBMC appropriately to align with this framework. We address this by treating DBMC as an interconnection of subsystems, where the estimation error and deviations in edge weights under perturbations serve as the state and the input of each subsystem, respectively. This approach facilitates the integration of DBMC into the small-gain framework, allowing us to derive the range of the

feedback gain that ensures the global exponential input-to-state stability (expISS) of DBMC, leading to improved stability results compared to existing works [9], [14]. The contribution of the paper can be summarized as twofold:

- While pre-specified finite time control strategies have been successfully applied to distributed consensus problems and certain types of distributed convex optimization problems [18], [19], [26], [27], this work, to the best of our knowledge, is the first attempt to extend such strategies to DBMC, which addresses the problem of finding the shortest path—a combinatorial optimization problem. The derived PT and PPT stabilization effects, essential for DBMC’s implementation in real applications, not only outperform existing results such as global asymptotic stability and regional exponential stability [9], [14], but also improve the stability results of the discretized version of DBMC, i.e., finite time convergence with dependency on initial states and structural aspects of the graph.
- As for DBMC itself, while existing works have demonstrated its global asymptotic stability or regional exponential stability, this work further establishes that the nominal DBMC is expISS by leveraging Lyapunov-based small-gain approaches. This result not only implies the global exponential stability of DBMC without perturbations, but also reveals its robustness in the presence of perturbations, as in this case its state error will decrease exponentially fast to a bound defined by the magnitude of the perturbations, regardless of the initial states.

The rest of the paper is organized as follows. Section II gives the notations and definitions, and states the problem of interest. Section III introduces PPT and PT control strategies on DBMC, respectively. Section IV presents the small-gain based analysis of the nominal DBMC. Section V provides the simulations, and Section VI concludes the paper.

II. PRELIMINARY KNOWLEDGE

As DBMC is a graph-based algorithm, in this section we first give the preliminary knowledge of graph theory. This section will also introduce the distributed biased min-consensus protocol and define key concepts that will facilitate our stability analysis.

We consider undirected graphs $G = (V, E)$ with $V = \{1, \dots, n\}$ the set of nodes and E the set of undirected edges. The set of neighbors of node $i \in V$ is denoted by $\mathcal{N}(i)$, and no node is deemed to be its own neighbor, i.e., $i \notin \mathcal{N}(i)$ for all $i \in V$. The weight of the edge between nodes i and j is denoted by w_{ij} and is assumed to be positive. Further, the set of source nodes is denoted by $S \subsetneq V$. Source and non-source nodes represent specific types of nodes in real-world applications. For example, in wireless sensor networks, the source node is the sink (base station), while the non-source node is the sensor that collects and transmits data to the sink via a designated path [28].

In addition to the graphical framework described above, we introduce the following notations, most of which will be used in Section IV. Define $\mathbb{R}, \mathbb{R}_+, \mathbb{Z}$ and \mathbb{Z}_+ as the set of real numbers, the set of nonnegative real numbers, the set of

integers and the set of nonnegative integers, respectively. For any $x \in \mathbb{R}^n$, $|x|$ and $|x|_\infty$ denote its ℓ_1 norm and ℓ_∞ norm, respectively. The space of measurable and essentially bounded functions is denoted by ℓ^∞ with norm $\|\cdot\|_\infty$.

The comparison functions \mathcal{K} and \mathcal{K}_∞ are defined as in [29]. We use the partial order induced by the component-wise ordering, i.e., for $x, y \in \mathbb{R}_+^n$, $x < y$ (resp. $x \leq y$) means $x_i < y_i$ (resp. $x_i \leq y_i$) for all $i \in \{1, \dots, n\}$, and $x \not\leq y$ means that there exists at least one index i such that $x_i < y_i$. A function $f: \mathbb{R} \rightarrow \mathbb{R}$ is of class C^2 if its second derivative is continuous. $\text{co}\{\cdot\}$ denotes the convex hull, i.e., for n points p_1, \dots, p_n , $\text{co}\{p_i \mid i \in \{1, \dots, n\}\} = \{\sum_{j=1}^n \lambda_j p_j : \lambda_j \geq 0 \text{ for all } j \text{ and } \sum_{j=1}^n \lambda_j = 1\}$.

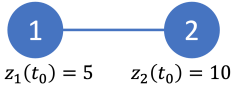


Fig. 1: Illustration of the necessity of the non-increasing property of $z_i(\cdot)$. In this graph consisting of two nodes, while applying $z_i(k+1) = \min_{j \in \mathcal{N}(i)} \{z_j(k)\}$, node 1 and node 2 will continuously exchange their initial value $z_1(t_0) = 5$ and $z_2(t_0) = 10$, thus min-consensus will never be achieved.

The definition of the *shortest path problem* considered in this paper is formally characterized as follows. Note that in this paper, multiple sources in the graph are allowed.

Definition 1. Consider an undirected graph $G = (V, E)$, the *shortest path problem* aims to find a path from each node i to its nearest source in S such that the sum of the weights of its constituent edges is minimized.

Let x_i^* denote the length/distance of the shortest path from node i to the source set. According to the Bellman's principle of optimality [5], x_i^* obeys the following recursion:

$$x_i^* = \begin{cases} 0, & i \in S \\ \min_{j \in \mathcal{N}(i)} \{x_j^* + w_{ij}\}, & i \notin S \end{cases} \quad (1)$$

Before turning to DBMC, we first revisit the rudiment of DBMC, specifically the discrete-time min-consensus protocol

$$z_i(k+1) = \min_{j \in \mathcal{N}(i) \cup \{i\}} \{z_j(k)\}, \quad (2)$$

where $z_i(k)$ represents the state of node i at the k -th time step. It has been shown in [2] that all nodes' states in (2) will converge to the minimum initial state within a finite number of iterations. In (2), i 's own state is considered, which is necessary to guarantee the convergence of (2). Without such condition, as shown in Figure 1, node 1 and node 2 may continuously exchange their initial states, preventing min-consensus from ever being achieved.

Let $t_0 = 0$ be the initial time and $x_i(t)$ be the state (estimated length of the shortest path from the source set at time t) of node i . Mimicking the style of (2) but using derivative instead and incorporating suitable edge weights, DBMC proposed in [4], [14] specifies the following recursion:

$$\dot{x}_i(t) = \begin{cases} 0, & i \in S \\ -\eta (x_i(t) - \min_{j \in \mathcal{N}(i)} \{x_j(t) + w_{ij}\}), & i \notin S \end{cases}, \quad (3)$$

where $x_i(0) = 0$ for all $i \in S$ and $\eta > 0$ is the feedback gain. The behavior of DBMC closely resembles the recursion (1) in the sense that the state of the source node is anchored at 0,

while that of a non-source node evolves using the minimum among the summations of its neighbors' states and the edge weights in between.

It is worthwhile noting that the distributed biased min-consensus protocol is fully distributed as each node only receives 1) the current states from its neighbors and 2) the edge weight transmitted by its neighbors or measured by the node itself. It has been proven in [4] and [14] respectively that DBMC can achieve global asymptotic stability and regional exponential stability (under the premise that all initial states are overestimates, i.e., $x_i(0) \geq x_i^*$ for all $i \in V \setminus S$).

To facilitate the analysis in the next section, we introduce the following definitions based on (1).

Definition 2. A minimizing j in the right hand side of the second bullet of (1) is called a *true parent node* of i . As i may have multiple true parent nodes, we use $\mathcal{P}(i)$ to denote the set of true parent nodes of node i . A source node does not have any true parent node.

Further, for an undirected graph $G = (V, E)$, consider a sequence of nodes such that the successor of each node is one of its true parent nodes. We define $\mathcal{D}(G)$, the *effective diameter* of G , as the longest length such a sequence can have in graph G . It has been proven that $\mathcal{D}(G)$ is finite and upper bounded by the diameter of graph G [12].

Another definition is needed to quantify the stability analysis.

Definition 3. We call a path from a node i to its nearest source $j \in S$ a *shortest path*, if it starts at i , ends with $j \in S$, and the successor of each node in the path is one of its true parent nodes. We call such a shortest path the *longest shortest path* if it has the most nodes among all shortest paths of i . The set \mathcal{F}_ℓ is the set of nodes whose longest shortest paths to the source set have $\ell + 1$ nodes.

Remark 1. Based on Definition 3, there holds $\mathcal{F}_0 = S$, $\mathcal{F}_{\mathcal{D}(G)+i} = \emptyset, \forall i \in \mathbb{Z}_+$, and $\mathcal{F}_i \neq \emptyset, \forall i \in \{0, \dots, \mathcal{D}(G) - 1\}$. Moreover, the following conditions hold:

$$\bigcup_{i \in \{0, \dots, \mathcal{D}(G)-1\}} \mathcal{F}_i = V \text{ and } \mathcal{F}_i \cap \mathcal{F}_j = \emptyset, \forall i \neq j. \quad (4)$$

(4) comes from the fact that each node $i \in V$ has a longest shortest path, and the number of nodes in such a path cannot exceed $\mathcal{D}(G)$ as defined in Definition 2. For any $i \in \mathcal{F}_\ell$ with $\ell \in \{1, \dots, \mathcal{D}(G) - 1\}$, i has a true parent node $j \in \mathcal{F}_{\ell-1}$.

Additionally, if i has multiple shortest paths to its nearest source with varying numbers of nodes, i only belongs to \mathcal{F}_ℓ with $\ell + 1$ the largest number of nodes among those paths.

We use Figure 2 to illustrate the above definitions. In the graph consisting of 9 nodes, there are 2 source nodes, node 1 and node 9 in red, and 7 non-source nodes in blue. Each edge weight is equal to 1, except for $w_{69} = 2$. The length of the shortest path from node 4 to its nearest source, node 1, is 2, which can be achieved via paths $4 \rightarrow 2 \rightarrow 1$ or $4 \rightarrow 3 \rightarrow 1$. Hence, the set of true parent nodes of node 4 is $\mathcal{P}(4) = \{2, 3\}$. The effective diameter of the graph is 3, as demonstrated by paths such as $6 \rightarrow 8 \rightarrow 9$.

Node 6 has two shortest paths to its nearest source, node

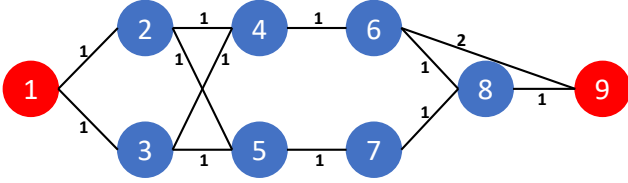


Fig. 2: Consider an undirected graph consisting of 7 non-source nodes and 2 source nodes. In this scenario, node 4 has 2 true parent nodes: node 2 and node 3. The effective diameter of the graph is 3. The longest shortest path of node 6 is $6 \rightarrow 8 \rightarrow 9$. Note that node 6 belongs to \mathcal{F}_2 but not to \mathcal{F}_1 .

9. These two paths are $6 \rightarrow 8 \rightarrow 9$ and $6 \rightarrow 9$. Among them, path $6 \rightarrow 8 \rightarrow 9$ is the longest shortest path of node 6. Consequently, by Definition 3, $6 \in \mathcal{F}_2$ but $6 \notin \mathcal{F}_1$.

To avoid trivialities the main assumption throughout the paper is summarized as follows.

Assumption 1. *The graph $G = (V, E)$ is connected and undirected, the source set $S \neq \emptyset$ and $S \subset V$, each edge weight is positive, and $t_0 = 0$ is the initial time.*

III. PRE-SPECIFIED FINITE TIME CONTROL STRATEGIES

In this section, we provide two control strategies for DBMC that enable PPT or PT stabilization of DBMC to the stationary value defined in (1). Unless explicitly stated otherwise, all proofs in this section are in the Appendix.

The following assumption holds throughout this section.

Assumption 2. *All non-source nodes have overestimated initial states, i.e., $x_i(0) \geq x_i^*$ for all $i \in V \setminus S$.*

Remark 2. *The above assumption is mild, as one can set the initial states sufficiently large to ensure it holds. Moreover, as will be shown later, the prescribed finite time for DBMC to converge is independent of the initial states under both proposed two strategies.*

A. The practical pre-specified finite time control strategy

The PPT control strategy is implemented by replacing the constant feedback gain in (3) with the time base generator (TBG) gain [22], [30], under which (5) is interpreted as

$$\dot{x}_i(t) = \begin{cases} 0, & i \in S \\ -\eta(t) (x_i(t) - \min_{j \in \mathcal{N}(i)} \{x_j(t) + w_{ij}\}), & i \notin S \end{cases}, \quad (5)$$

where the TBG gain $\eta(t)$ obeys

$$\eta(t) = \frac{\dot{\varepsilon}(t - k \cdot T_s)}{1 - \varepsilon(t - k \cdot T_s) + \delta}, \quad \forall t \in [k \cdot T_s, (k+1) \cdot T_s), \quad (6)$$

with $k \in \mathbb{Z}_+$, T_s a pre-specified time constant, $\varepsilon(t)$ a TBG and $0 < \delta \ll 1$. Specifically, $\varepsilon(t)$ has the following properties:

- $\varepsilon(t)$ is at least C^2 on $(0, +\infty)$;
- $\varepsilon(t)$ is continuous and non-decreasing from an initial value $\varepsilon(0) = 0$ to a terminal value $\varepsilon(T_s) = 1$, where $T_s < +\infty$ is a pre-specified time instant;
- $\dot{\varepsilon}(0) = \dot{\varepsilon}(T_s) = 0$ and $\varepsilon(t) = 1$ when $t > T_s$.

A suitable example of TBG with $T_s = 4$ could be

$$\varepsilon(t) = \begin{cases} \frac{10}{4^6} t^6 - \frac{24}{4^5} t^5 + \frac{15}{4^4} t^4, & 0 \leq t \leq T_s \\ 1, & t > T_s \end{cases}, \quad (7)$$

Remark 3. *Unlike the TBG used in [22], [30], this paper employs a truncated version of TBG repeatedly. Since $\varepsilon(t)$ is of class C^2 on $(0, +\infty)$ and $\dot{\varepsilon}(T_s) = 0$, the TBG gain $\eta(t)$ in (5) is continuous, bounded and nonnegative on $[0, +\infty)$.*

We first provide the definition of practical pre-specified finite time stability for (5).

Definition 4. ([17], [22]): *We say (5) achieves practical pre-specified finite time stability if for all $i \in V$, $|x_i(t) - x_i^*| \leq c$ for $t \geq T_s$, with x_i^* defined in (1), T_s a user-defined time independent of the initial conditions and c an adjustable positive number.*

As $\eta(t)$ in (5) is bounded and continuous on $[0, +\infty)$, (5) admits a unique solution per the following theorem.

Theorem 1. *Suppose Assumption 1 holds, (5) has a unique solution for $t \in [0, +\infty)$.*

Before proceeding, we introduce the following technical result regarding our TBG gain $\eta(t)$.

Lemma 1. *Consider the differential equation*

$$\dot{y}(t) = -\eta(t)y(t), y(0) = y_0, t \in [0, T_s], \quad (8)$$

where $\eta(t)$ is defined in (6). Then $y(T_s) = \frac{\delta}{1+\delta}y_0$.

Define $e_i(t)$ as the error between $x_i(t)$, the state of i , and its stationary value x_i^* as

$$e_i(t) = x_i(t) - x_i^*, \quad \forall i \in V. \quad (9)$$

With $e_i(t)$ defined in (9), magnitudes of the largest state error and the least state error are given by

$$V^+(t) := \max \{0, \max_{i \in V} \{e_i(t)\}\} \quad (10)$$

and

$$V^-(t) := \max \{0, -\min_{i \in V} \{e_i(t)\}\}, \quad (11)$$

respectively. Apparently $V^+(t) \geq 0, V^-(t) \geq 0$ for all $t \geq 0$, and $V^+(t) = V^-(t) = 0$ implies $e_i(t) = 0$ for all $i \in V$, i.e., all states converge to their stationary values at time t .

As $V^+(t)$ and $V^-(t)$ defined above are non-smooth functions, we need the following two sets to calculate their Clarke's generalized derivatives [4], [31]. Define $\mathcal{K}(t)$ as the set comprising nodes for which state errors equal $V^+(t)$,

$$\mathcal{K}^+(t) = \{i \in V \mid e_i(t) = V^+(t)\}. \quad (12)$$

Similarly, $\mathcal{K}^-(t)$, the set comprising nodes which achieve the least state error, is defined as

$$\mathcal{K}^-(t) = \{i \in V \mid e_i(t) = -V^-(t)\}. \quad (13)$$

Both $V^+(t)$ and $V^-(t)$ are non-increasing, per the following two lemmas.

Lemma 2. *Suppose Assumption 1 holds, with $\mathcal{K}^+(t)$ defined in (12), $V^+(t)$ defined in (10) obeys $\dot{V}^+(t) \leq 0$ for all $t \geq 0$.*

Proof. According to Clarke's generalized derivative [4], [31] (detailed proof can be referred to sections 2.2 and 2.3 in [31]), $\dot{V}^+(t) = \text{co}\{\dot{e}_i(t) \mid i \in \mathcal{K}^+(t)\}$.

We need to consider three cases: 1) $\mathcal{K}^+(t) \cap S = \emptyset$, i.e., $\exists i \in V \setminus S, e_i(t) > 0$; 2) $S = \mathcal{K}^+(t)$, i.e., $\forall i \in V \setminus S, e_i(t) < 0$; 3) $S \subsetneq \mathcal{K}^+(t)$, i.e., $\forall i \in V \setminus S, e_i(t) \leq 0$ and $\exists i \in V \setminus S, e_i(t) = 0$.

In the first case, there holds $V^+(t) > 0$ as $\mathcal{K}^+(t) \cap S = \emptyset$, it follows from (5) and (9) that

$$\begin{aligned} \dot{V}^+(t) &= \sum_{i \in \mathcal{K}^+(t)} \lambda_i \eta(t) (-x_i(t) + \min_{k \in \mathcal{N}(i)} \{x_k(t) + w_{ik}\}) \\ &= \sum_{i \in \mathcal{K}^+(t)} \lambda_i \eta(t) (-x_i^* - e_i(t) + \min_{k \in \mathcal{N}(i)} \{x_k(t) + w_{ik}\}) \\ &= \sum_{i \in \mathcal{K}^+(t)} \lambda_i \eta(t) (-x_j^* - w_{ij} - e_i(t) + \min_{k \in \mathcal{N}(i)} \{x_k(t) + w_{ik}\}) \end{aligned} \quad (14)$$

$$\leq \sum_{i \in \mathcal{K}^+(t)} \lambda_i \eta(t) (-x_j^* - w_{ij} - e_i(t) + x_j(t) + w_{ij}) \quad (15)$$

$$\begin{aligned} &= \sum_{i \in \mathcal{K}^+(t)} \lambda_i \eta(t) (e_j(t) - e_i(t)) \\ &\leq 0 \end{aligned} \quad (16)$$

where in (14) we assume $j \in \mathcal{P}(i)$, (15) uses the fact that $\eta(t) \geq 0$ and $\lambda_i \geq 0$, and (16) uses the fact that $\eta(t) \geq 0$, $\lambda_i \geq 0$ and $e_i(t) \geq e_j(t)$ for all $j \in V$ as $i \in \mathcal{K}^+(t)$.

In the second case, we have $V^+(t) = 0$ as $S = \mathcal{K}^+(t)$, it follows from (5) and (9) that $\dot{V}^+(t) = \sum_{i \in S} \lambda_i \dot{e}_i(t) = 0$ with $\lambda_i \geq 0$ and $\sum_{i \in S} \lambda_i = 1$ for $i \in S$.

For case 3), it follows from the above two cases that

$$\begin{aligned} \dot{V}^+(t) &= \sum_{i \in \mathcal{K}^+(t)} \lambda_i \dot{e}_i(t) = \sum_{k \in S} \lambda_k \dot{e}_k(t) + \sum_{j \in \mathcal{K}^+(t) \setminus S} \lambda_j \dot{e}_j(t) \\ &= \sum_{j \in \mathcal{K}^+(t) \setminus S} \lambda_j \dot{e}_j(t) \leq 0, \end{aligned} \quad (17)$$

where the equality in (17) uses the fact that $\dot{e}_k(t) = 0$ for all $k \in S$, and the inequality in (17) uses the fact that $0 \leq \lambda_j \leq 1$ and (14)-(16). Therefore, our proof is complete. ■

To prove that $V^-(t)$ is also monotonically non-increasing, we first define $\mathcal{P}_i(t)$, the set of current parent nodes of node i , as follows:

$$\mathcal{P}_i(t) = \begin{cases} \emptyset, & i \in S \\ \arg \min_{j \in \mathcal{N}(i)} \{x_j(t) + w_{ij}\}, & i \notin S \end{cases} \quad (18)$$

Lemma 3. *Suppose Assumption 1 holds, with $\mathcal{K}^-(t)$ defined in (13), $V^-(t)$ defined in (11) obeys $\dot{V}^-(t) \leq 0$ for all $t \geq 0$.*

Proof. By Clarke's generalized derivative, $\dot{V}^-(t) = \text{co}\{-\dot{e}_i(t) \mid i \in \mathcal{K}^-(t)\}$.

We consider the three cases: 1) $\mathcal{K}^-(t) \cap S = \emptyset$, i.e., $V^-(t) > 0$; 2) $S = \mathcal{K}^-(t)$; 3) $S \subsetneq \mathcal{K}^-(t)$.

For the first case, it follows from (5) and (9) that

$$\begin{aligned} \dot{V}^-(t) &= \sum_{i \in \mathcal{K}^-(t)} \lambda_i \eta(t) (x_i(t) - \min_{k \in \mathcal{N}(i)} \{x_k(t) + w_{ik}\}) \\ &= \sum_{i \in \mathcal{K}^-(t)} \lambda_i \eta(t) (x_i^* + e_i(t) - x_k(t) - w_{ik}) \end{aligned} \quad (19)$$

$$\leq \sum_{i \in \mathcal{K}^-(t)} \lambda_i \eta(t) (x_k^* + w_{ik} + e_i(t) - x_k(t) - w_{ik}) \quad (20)$$

$$\begin{aligned} &= \sum_{i \in \mathcal{K}^-(t)} \lambda_i \eta(t) (e_i(t) - e_k(t)) \\ &\leq 0 \end{aligned} \quad (21)$$

where in (19) we assume $k \in \mathcal{P}_i(t)$, (20) uses (1) and the fact that $\eta(t) \geq 0$, $\lambda_i \geq 0$, and (21) uses the fact that $\eta(t) \geq$

0 , $\lambda_i \geq 0$ and $e_i(t) \leq e_j(t)$ for all $j \in V$ as $i \in \mathcal{K}^-(t)$.

Similar to the arguments in Lemma 2, there holds $V^-(t) = 0$ in case 2) and $\dot{V}^-(t) \leq 0$ in case 3), completing our proof. ■

Lemma 2 and Lemma 3 indicate that both the largest overestimate and the least underestimate are non-increasing. Note that neither lemma requires Assumption 2. Under Assumption 2, we further get the following appealing result.

Lemma 4. *Suppose Assumptions 1 and 2 hold. With $x_i(t)$ and x_i^* defined in (5) and (1), respectively, there holds $x_i(t) \geq x_i^*$ for all $i \in V$ and $t \geq 0$.*

Proof. In this case $V^-(0) = 0$. As $V^-(t) \geq 0$ for all $t \geq 0$ by its definition and $\dot{V}^-(t) \leq 0$ by Lemma 3, we have $V^-(t) = 0$ for all $t \geq 0$, and thus our claim follows. ■

The following lemma characterizes the upper bound for the state error of (5). The basic pattern is that, once the state error of the true parent node of some node is upper bounded at a given time, T_s time later the node's own state error will drop below an upper bound. Both bounds can be defined by the maximum initial state and the adjustable parameter δ in (6). To this end, we first define the maximum initial state error as

$$e_{\max}(0) = \max_{i \in V} \{e_i(0)\}. \quad (22)$$

Lemma 5. *Suppose Assumptions 1 and 2 hold, consider (5), with $e_i(t)$, T_s and \mathcal{F}_ℓ defined in (9), (6) and Definition 3, respectively. Then for all $i \in \mathcal{F}_\ell$ with $\ell \in \{1, \dots, \mathcal{D}(G) - 1\}$ there holds for $t \geq \ell T_s$*

$$e_i(t) \leq \ell \frac{\delta}{1 + \delta} e_{\max}(0), \quad (23)$$

where $0 < \delta \ll 1$ is an adjustable parameter given in (6).

As the lower bound of the state error has been determined in Lemma 4 under Assumption 2, the following theorem completes this subsection by demonstrating the PPT stabilization of (5) as defined in Definition 4.

Theorem 2. *Suppose Assumptions 1 and 2 hold, consider (5), with $e_i(t)$, T_s and \mathcal{F}_ℓ defined in (9), (6) and Definition 3, respectively. Then for all $i \in \mathcal{F}_\ell$ with $\ell \in \{1, \dots, \mathcal{D}(G) - 1\}$ there holds for $t \geq (\mathcal{D}(G) - 1)T_s$*

$$|e_i(t)| \leq \ell \frac{\delta}{1 + \delta} e_{\max}(0), \quad (24)$$

where $0 < \delta \ll 1$ is an adjustable parameter given in (6).

Proof. This is a direct result of Lemma 4 and Lemma 5. ■

Theorem 2 reflects that, under PPT control strategy, each node's state will converge to the neighborhood of its stationary value within the settling time. Such settling time is prescribed without dependence on the initial state. Though a state disagreement always exists after the prescribed time, one can adjust the parameter δ in the TBG to reduce the discrepancy to a desired level.

B. The pre-specified finite time control strategy

A gap between the state and its stationary value always exists under PPT control strategy introduced in the previous

subsection. To remedy such an imperfection, in this subsection PT control strategy is presented such that the state error will diminish exactly to zero within a prescribed time.

Similar to PPT control strategy, PT control strategy is achieved through replacing the feedback gain η in (3) with a time-varying scaling function $\bar{\eta}(t)$ such that (3) becomes

$$\dot{x}_i(t) = \begin{cases} 0, & i \in S \\ -\bar{\eta}(t)(x_i(t) - \min_{j \in \mathcal{N}(i)} \{x_j(t) + w_{ij}\}), & i \notin S \end{cases}, \quad (25)$$

where

$$\bar{\eta}(t) = \begin{cases} \gamma + 2\frac{\dot{\rho}(t)}{\rho(t)}, & t \in [0, \bar{T}_s) \\ 0, & t \geq \bar{T}_s \end{cases}, \quad (26)$$

with $\gamma > 0$ and $\rho(t)$ obeying

$$\rho(t) = \frac{\bar{T}_s^{1+h}}{(\bar{T}_s - t)^{1+h}}, \quad t \in [0, \bar{T}_s) \quad (27)$$

where \bar{T}_s is a prescribed time constant and $h \in \mathbb{Z}_+$ can be chosen as $h > \mathcal{D}(G)/2$.

Remark 4. It is important to note that h in (27) does not require the exact value of $\mathcal{D}(G)$, but rather an upper bound of it. Such requirements are commonly encountered in pre-specified finite time control frameworks. For instance, in the context of pre-specified control for distributed consensus problems [19] and distributed convex optimization problems with consensus constraints [26], [27], upper bounds on global information, such as the number of nodes or the second smallest eigenvalue of the Laplacian matrix, are also needed. As $\mathcal{D}(G)$ is upper bounded by the graph's diameter or number of nodes, practical implementations aiming for fully distributed realization can use the lower layers of the network stack (e.g., 128 bits in IPv6) to obtain an upper bound for the number of nodes. As will be demonstrated later, the magnitude of h does not influence the stability analysis once it exceeds $\mathcal{D}(G)/2$.

Remark 5. Unlike [18], where the time-varying scaling function is constructed by reusing the first bullet of (26), the time-varying scaling function used here is designed to reduce to zero after the prescribed time instant. As will be shown later, this setup ensures the continuity of $\dot{x}_i(t)$, which in turn guarantees the existence and continuity of $x_i(t)$, the solution to (25).

The formal definition of pre-specified finite time stability of (25) is given below.

Definition 5. ([17], [18]): We say (25) achieves pre-specified finite time stability if for all $i \in V$, $x_i(t) = x_i^*$ for $t \geq \bar{T}_s$, with x_i^* defined in (1), \bar{T}_s a user-defined time independent of the initial conditions.

We first give a generalized result of Lemma 2 in [18].

Lemma 6. Consider the differential equation

$$\dot{y}(t) = -\left(\gamma + \alpha \frac{\dot{\rho}(t)}{\rho(t)}\right) y(t), \quad t \in [t_0, \bar{T}_s), \quad (28)$$

where $\rho(t)$ is defined in (27), $\gamma, \alpha > 0$ and $0 \leq t_0 < \bar{T}_s$. Then $y(t) = \rho^{-\alpha}(t)\rho^\alpha(t_0)e^{-\gamma(t-t_0)}y(t_0)$ for $t \in [t_0, \bar{T}_s)$.

By definition of $\rho(t)$, Lemma 6 implies that

$$\lim_{t \rightarrow \bar{T}_s^-} y(t) = 0. \quad (29)$$

Let the state error $e_i(t)$, the greatest overestimate $V^+(t)$ and the least underestimate $V^-(t)$ be in the form of (9), (10) and (11), respectively, with $x_i(t)$ there being replaced by the one defined in (25). The next lemma summarizes their properties under PT control strategy, over the interval $[0, \bar{T}_s)$.

Lemma 7. Suppose Assumption 1 holds, $V^+(t)$ and $V^-(t)$ defined above obey $\dot{V}^+(t) \leq 0$ and $\dot{V}^-(t) \leq 0$ for $t \in [0, \bar{T}_s)$. Moreover, suppose Assumption 2 also holds, then $x_i(t) \geq x_i^*$ for all $i \in V$ and $t \in [0, \bar{T}_s)$.

Proof. As $\bar{\eta}(t) > 0$ over $[0, \bar{T}_s)$, the proof follows directly from those of Lemma 2 to Lemma 4. \blacksquare

With the lower bound of the state being determined in Lemma 7, the left-hand limit of each state at \bar{T}_s is given in the following lemma, as the first step to calculate the left-hand limit of the derivative of each state.

Lemma 8. Suppose Assumptions 1 and 2 hold, consider (25), with x_i^* defined in (1), for all $i \in V \setminus S$, there holds

$$\lim_{t \rightarrow \bar{T}_s^-} x_i(t) = x_i^*. \quad (30)$$

Although Lemma 8 shows that each state converges to its stationary value as t approaches \bar{T}_s , we still need to prove the continuity of each state on $[0, +\infty)$ to establish the finite time convergence of (25). A simple and feasible approach is to show the continuity of its derivative, specifically by proving that the left-hand limit of $\dot{x}_i(t)$ at \bar{T}_s is 0.

The following lemma first proves the continuity of derivatives of the states for nodes in \mathcal{F}_1 , while providing the upper bounds for state errors of the remaining nodes over $[0, \bar{T}_s)$.

Lemma 9. Suppose Assumptions 1 and 2 hold, consider (25), with $\rho(t)$ and \mathcal{F}_ℓ defined in (27) and Definition 3, respectively, there holds

$$\lim_{t \rightarrow \bar{T}_s^-} \dot{x}_i(t) = \dot{e}_i(t) = 0, \quad \forall i \in \mathcal{F}_1, \quad (31)$$

and for $t \in [0, \bar{T}_s)$

$$e_i(t) \leq \frac{(\bar{T}_s - t)^{2h+3-\ell}}{\bar{T}_s^{2h+3-\ell}} (e^{-\gamma t} e_i(0) + c_i), \quad \forall i \in \mathcal{F}_\ell \quad (32)$$

for $\ell \in \{2, \dots, \mathcal{D}(G) - 1\}$, with some constant $c_i > 0$.

With the upper bound of state error provided in Lemma 9, we then use Squeeze theorem [32] to prove the continuity of derivatives of the states for the remaining nodes.

Lemma 10. Suppose Assumptions 1 and 2 hold, with \mathcal{F}_ℓ defined in Definition 3, there holds

$$\lim_{t \rightarrow \bar{T}_s^-} \dot{x}_i(t) = \dot{e}_i(t) = 0, \quad \forall i \in \mathcal{F}_\ell \quad (33)$$

for $\ell \in \{2, \dots, \mathcal{D}(G) - 1\}$.

The pre-specified finite time stability of (25) follows as a byproduct of the above lemma.

Theorem 3. Suppose Assumptions 1 and 2 hold, consider (25), with x_i^* defined in (1), then for all $i \in V$, $x_i(t)$ is continuous on $[0, +\infty)$ and

$$x_i(t) = x_i^*, \quad \forall i \in V \text{ and } \forall t \geq \bar{T}_s. \quad (34)$$

Proof. The continuity of $x_i(t)$ on $[0, +\infty)$ is guaranteed by Lemma 9 and Lemma 10, leading to $x_i(\bar{T}_s) = x_i^*$ for all

$i \in V$ by (30) in Lemma 8. Further, as $\dot{x}_i(t) = \dot{e}_i(t) = 0$ for all $t \geq \bar{T}_s$, we have $x_i(t) = x_i^*$ for all $i \in V$ and $t \geq \bar{T}_s$. ■

As shown in Theorem 3, PT control strategy ensures finite time convergence without dependence on the initial states. Moreover, the control input, i.e., the right-hand side of (25), remains continuous and bounded even when the feedback gain approaches infinity at the presetting time instant. As a result, PT control strategy generates continuously differentiable distance estimate $x_i(t)$ at all times.

The theorem below completes this section by showing that the solution to (25), as established in Theorem 3, is also unique, by leveraging the fact that each state resides within a compact set for $t \geq 0$.

Theorem 4. *Suppose Assumptions 1 and 2 hold, (25) admits a unique solution for $t \in [0, +\infty)$.*

Proof. From the proof of Theorem 1 and the fact that $\bar{\eta}(t)$ defined in (26) is continuous on $[0, \bar{T}_s)$, $f_i(t, \tilde{x}) = -\bar{\eta}(t)(\tilde{x}_i - \min_{j \in \mathcal{N}(i)} \{\tilde{x}_j + w_{ij}\})$ with $\tilde{x} = [\tilde{x}_1, \dots, \tilde{x}_n]^\top \in \mathbb{R}^n$ and $i \in \{1, \dots, n\}$, is Lipschitz continuous with respect to its second argument for all $t \in [0, t_1]$, with $t_1 < \bar{T}_s$. Also, $f_i(\cdot, \tilde{x})$ is continuous on $[0, t_1]$ for all $\tilde{x} \in \mathbb{R}^n$. Further, define a compact set $P_i = [x_i^*, x_i^* + e_{\max}(0)]$ for all $i \in V$ with $e_{\max}(0)$ the largest initial state error. As the largest state error is non-increasing and $x_i(t) \geq x_i^*$ for all $t \in [0, \bar{T}_s)$ by Lemma 7, as well as $x_i(t)$ is continuous on $[0, +\infty)$ and $x_i(t) = x_i^*$ for $t \geq \bar{T}_s$ by Theorem 3, there holds that $x_i(t)$ remains entirely within P_i once $x_i(0) \in P_i$. Then it follows from Theorem 2.39 in [33] that the solution to (25) is unique. ■

IV. SMALL-GAIN BASED ANALYSIS

In this section, we revisit the nominal model of the distributed biased min-consensus protocol represented by (3). We will demonstrate that (3) is globally exponentially input-to-state stable (per Definition 2.68 in [34]) when its edge weights are subject to persistent perturbations, i.e., the edge weight w_{ij} in (3) is perturbed from its nominal value and becomes time-varying. Under such a perturbation (3) can be expressed as

$$\dot{x}_i(t) = \begin{cases} 0, & i \in S \\ -\eta(x_i(t) - \min_{j \in \mathcal{N}(i)} \{x_j(t) + w_{ij}(t)\}), & i \notin S \end{cases} \quad (35)$$

We assume that the edge weights are continuous and bounded under perturbation, which includes, but is not limited to the additive perturbation on the edge weights (i.e., $w_{ij}(t) = w_{ij} + \epsilon_{ij}(t)$ with $\epsilon_{ij}(t) > 0$) considered in [14], and bounded stochastic noise. Specifically, we assume $\forall i \in V$ and $j \in \mathcal{N}(i)$

$$0 < w_{\min} \leq w_{ij}(t) \leq w_{\max}, \forall t \geq 0. \quad (36)$$

Note that (36) allows asymmetric perturbations, i.e., $w_{ij}(t) \neq w_{ji}(t)$ is allowed.

Before proceeding with the stability analysis, we first convert (35) into a nonlinear dynamical system. We continue to use the notions of state error $e_i(t)$ and node i 's set of current parent nodes $\mathcal{P}_i(t)$, as defined in (9) and (18), respectively, with $x_i(t)$ as described in (35). We further define

$$u_{ij}(t) = w_{ij}(t) - w_{ij} \quad (37)$$

as the deviation of the edge weight from its nominal value. Then (35) can be rewritten as $\dot{e}_i(t) = 0$ if $i \in S$ and

$$\dot{e}_i(t) = -\eta(x_i + e_i(t) - \min_{j \in \mathcal{N}(i)} \{e_j(t) + x_j + u_{ij}(t) + w_{ij}\}), \text{ if } i \notin S, \quad (38)$$

with x_i^*, x_j^* and w_{ij} the structural aspects of the graph G . By taking $e_i(t)$ and $u_{ij}(t)$ as the state and the input, respectively, (38) can be further described by a nonlinear map $f_i : \mathbb{R}^{|\mathcal{N}(i)|+1} \times \mathbb{R}^{|\mathcal{N}(i)|} \rightarrow \mathbb{R}$, i.e.,

$$\dot{e}_i(t) = f_i(e_i(t), e_{i_1}(t), \dots, e_{i_{|\mathcal{N}(i)|}}(t), u_i(t)) \quad (39)$$

where $i_\ell \in \mathcal{N}(i)$ for $\ell \in \{1, \dots, |\mathcal{N}(i)|\}$ and $u_i(t) = [u_{i,i_1}(t), \dots, u_{i,i_{|\mathcal{N}(i)|}}(t)]^\top \in \mathbb{R}^{|\mathcal{N}(i)|}$. The overall system can be defined by the following composite nonlinear map $F : \mathbb{R}^n \times \mathbb{R}^{2|E|} \rightarrow \mathbb{R}^n$

$$\dot{e}(t) = F(e(t), u(t)) \quad (40)$$

where $e(t) = [e_1(t), \dots, e_n(t)]^\top \in \mathbb{R}^n$ and $u(t) = (u_{ij}(t))_{i \in V, j \in \mathcal{N}(i)} \in \mathbb{R}^{2|E|}$. Also, $F(0, 0) = 0$ as in this case $\dot{e}_i(t) = e_i(t) = 0$ for all $i \in V$ by (1) and (35).

It can be seen from (38), (39) and (40) that F is continuous in t . Additionally, since $\eta > 0$ is a constant feedback gain, it follows from the proof of Theorem 1 that F is globally Lipschitz continuous with respect to its first argument. Consequently, (40) admits a unique solution over $t \in [0, +\infty)$ [29]. Therefore, global exponential input-to-state stability can be defined for (40), with details given below.

Definition 6. (*[34]*): (40) is said to be globally exponentially input-to-state stable (expISS) if

- for all the initial state $e(0) \in \mathbb{R}^n$ and all the input $u \in \ell^\infty(\mathbb{R}^{2|E|})$, the corresponding solution to (40) exists and is unique on $[0, +\infty)$;
- there exist $c, p > 0$ and $\lambda_u \in \mathcal{K}$ such that, for all the initial state $e(0) \in \mathbb{R}^n$, $u \in \ell^\infty(\mathbb{R}^{2|E|})$, there holds

$$|e(t)| \leq ce^{-pt}|e(0)| + \lambda_u(\|u\|_\infty), \forall t \geq 0. \quad (41)$$

Obviously (40) is globally exponentially stable (per Definition 4.5 in [29]) with 0-input once it is expISS. A direct method to demonstrate the expISS of (40) is to show the existence of an exponential ISS Lyapunov function (refer to Definition 6.28 and Proposition 6.29 in [34] for more details), which is central in this section.

Definition 7. A continuous function $V : \mathbb{R}^n \rightarrow \mathbb{R}_+$ is called an exponential ISS Lyapunov function (expISS Lyapunov function) for (40) if there exist constants $\underline{\omega}, \bar{\omega}, b, \kappa > 0$ and $\chi \in \mathcal{K}_\infty$ such that for $x \in \mathbb{R}^n$ and all $u \in \ell^\infty(\mathbb{R}^{2|E|})$

$$\underline{\omega}|x|^b \leq V(x) \leq \bar{\omega}|x|^b, \quad (42)$$

$V(x) \geq \chi(\|u(t)\|) \implies \forall \xi \in \text{co}\{\bar{\xi} : \exists x_k \rightarrow x : \nabla V(x_k) \text{ exists and } \nabla V(x_k) \rightarrow \bar{\xi}\}, \dot{V}(x) := \langle \xi, \dot{x}(t) \rangle \leq -\kappa V(x).$ (43)

where $\langle \cdot, \cdot \rangle$ denotes the standard scalar product in \mathbb{R}^n .

Remark 6. It should be noted that the upper right-hand Dini derivative is used in [34] for (43), while here we use the Clarke's generalized derivative instead. As in this paper we will adopt ℓ_1 norm $\|\cdot\|$ as our candidate expISS Lyapunov function, these two derivatives remain to be same when the argument of V is nonzero. In particular, if V takes $e(t)$ defined

in (40) as the argument and $e(t) = 0$, as F given in (40) obeys $F(0, 0) = 0$, it can be readily verified that when the condition in (43) holds, i.e., $V(e(t)) = |e(t)| \geq \chi(|u(t)|)$, then $\dot{V}(e(t)) = 0 = -\kappa V(e(t))$ under both types of derivatives.

The above expISS Lyapunov function is called an implication-form expISS Lyapunov function. Another candidate to guarantee expISS is the dissipative-form expISS Lyapunov function, which satisfies (42) with (43) being replaced by $\dot{V}(x) \leq -\epsilon V(x) + \gamma(|u(t)|)$ for some $\epsilon > 0$ and $\gamma \in \mathcal{K}_\infty$. It has been shown in Proposition 6.29 of [34] that the dissipative-form expISS Lyapunov function implies the implication-form one, and they both imply the expISS of (35).

We summarize the assumption throughout this section.

Assumption 3. Each edge weight is perturbed from its nominal value and obeys (36). All initial states are nonnegative.

Remark 7. Unlike the requirements that all states need to be overestimates as assumed in the previous section or in [14], this section only assumes that all initial states are nonnegative. This assumption is merely used to facilitate the stability analysis. Indeed, by using the absolute value of received states from neighbors, i.e., (35) becomes

$$\dot{x}_i(t) = \begin{cases} 0, & i \in S \\ -\eta(x_i(t) - \min_{j \in \mathcal{N}(i)} \{|x_j(t)| + w_{ij}(t)\}), & i \notin S \end{cases}, \quad (44)$$

all states will become nonnegative after a finite time, and (44) reduces to (35) thereafter. Proof of this claim is provided in the Appendix.

Our proof primarily relies on the Lyapunov-based small-gain theorem, as introduced in Theorem 5.3 and Corollary 5.6 in [24], which addresses the ISS of interconnected subsystems. The establishment of this theorem requires two key conditions: (1) each subsystem possesses a Lyapunov-like function similar to (42, 43); and (2) these Lyapunov-like functions satisfy a cyclic small-gain condition, which allows the formulation of an ISS Lyapunov function for the overall system, thereby ensuring the ISS. Along this line, the key steps in our proof are divided into two parts. In Lemma 11, by using the estimation error $e_i(t)$ as the state and the deviations of edge weights $u(t)$ as the input, we demonstrate that each node admits a function that resembles the expISS Lyapunov function defined in Definition 7, thereby satisfying condition (1). In Lemma 12, we prove that these Lyapunov-like functions indeed satisfy the cyclic small-gain condition, thereby fulfilling condition (2).

Recall the stationary value defined in (1). Given that numbers of nodes and edges in graph G are both finite, there must exist a $\zeta \in (0, 1)$ such that for all $i \in V$ with $\mathcal{N}(i) \setminus \mathcal{P}(i) \neq \emptyset$,

$$\frac{x_i^*}{x_l^* + w_{il}} \leq \zeta, \quad \forall l \in \mathcal{N}(i) \setminus \mathcal{P}(i). \quad (45)$$

We exemplify (45) using Figure 2. For node 8, we have $\mathcal{N}(8) = \{6, 7, 9\}$ and $\mathcal{P}(8) = \{9\}$, and there holds $\frac{x_8^*}{x_6^* + w_{68}} = \frac{x_8^*}{x_7^* + w_{78}} = \frac{1}{3}$, and it can be verified that (45) holds for any node i satisfying $\mathcal{N}(i) \setminus \mathcal{P}(i) \neq \emptyset$ in Figure 2 with $\zeta = \frac{2}{3}$.

We first show that the state error of each node admits an expISS Lyapunov-like trajectory.

Lemma 11. Suppose Assumptions 1 and 3 hold, consider (35),

with ζ defined in (45), $e_i(t)$ and $\mathcal{P}_i(t)$ the state error and the set of current parent nodes of node i under (35), respectively. Let $V_i(\cdot) = |\cdot|$ for $i \in V$. The following conditions hold:

- If $i \in S$, then

$$V_i(e_i(t)) = 0, \quad \forall t \geq 0. \quad (46)$$

- If $i \notin S$ and $V_i(e_i(t)) \geq \max_{j \in \{1, \dots, n\}} \{\lambda_{ij} V_j(e_j(t))\} + \lambda_{iu} |u(t)|$, then

$$\dot{V}_i(e_i(t)) \leq -(\eta - 1)V_i(e_i(t)), \quad \forall t \geq 0, \quad (47)$$

where $\lambda_{ij} = \eta$ when j is a true parent node of i and $\lambda_{ij} = \zeta\eta$ otherwise, and $\lambda_{iu} = \eta$.

With state error trajectories characterized in (46) and (47), we define the $n \times n$ gain matrix $\Gamma : (\bar{\lambda}_{ij})_{i,j \in \{1, \dots, n\}}$ with the element $\bar{\lambda}_{ij}$ in the i -th row and j -th column obeying $\bar{\lambda}_{ij} = 0.5/\eta^{\mathcal{D}(G)-1}$ for all $i \in S$ and $j \in \{1, \dots, n\}$, and $\bar{\lambda}_{ij} = \lambda_{ij}$ otherwise, with λ_{ij} defined in (47), i.e.,

$$\bar{\lambda}_{ij} = \begin{cases} \zeta\eta, & i \notin S, j \notin \mathcal{P}(i) \\ \eta, & i \notin S, j \in \mathcal{P}(i) \\ 0.5/\eta^{\mathcal{D}(G)-1}, & i \in S \end{cases} \quad (48)$$

with $\mathcal{P}(i)$ and $\mathcal{D}(G)$ in (48) the set of i 's true parent nodes and the effective diameter of G , respectively. The corresponding $n \times n$ adjacency matrix $A_\Gamma : (a_{ij})_{i,j \in \{1, \dots, n\}}$ is defined by

$$a_{ij} = \begin{cases} 1 & \bar{\lambda}_{ij} \neq 0 \\ 0 & \text{otherwise} \end{cases}. \quad (49)$$

With $V_i := |\cdot|$ for $i \in V$, it follows from (46) and (47) that $V_i(e_i(t)) \geq \max\{\bar{\lambda}_{i1} V_1(e_1(t)), \dots, \bar{\lambda}_{in} V_n(e_n(t))\} + \eta|u(t)| \implies \dot{V}_i(e_i(t)) \leq -(\eta - 1)V_i(e_i(t)), \quad \forall i \in V. \quad (50)$

By transforming (46, 47) to (50), it follows that each node indeed admits a Lyapunov-like function close to (42, 43), where $V_j(e_j(t))$ with $j \in \{1, \dots, n\}$ and $u(t)$ act as inputs.

A gain matrix Γ is called irreducible if and only if the graph resulting from its corresponding adjacency matrix is strongly connected [24], [35]. Since A_Γ has no zero elements by (48) and (49), the gain matrix Γ defined by (48) is irreducible.

Define the map motivated by the gain matrix Γ as

$$\Gamma_\oplus : \mathbb{R}_+^n \rightarrow \mathbb{R}_+^n, \quad \begin{bmatrix} s_1 \\ \vdots \\ s_n \end{bmatrix} \mapsto \begin{bmatrix} \max_{k \in \{1, \dots, n\}} \{\bar{\lambda}_{1k} s_k\} \\ \vdots \\ \max_{k \in \{1, \dots, n\}} \{\bar{\lambda}_{nk} s_k\} \end{bmatrix}, \quad (51)$$

as well as the diagonal operator $D : \mathbb{R}_+^n \rightarrow \mathbb{R}_+^n$ as

$$D : \mathbb{R}_+^n \rightarrow \mathbb{R}_+^n, [s_1, \dots, s_n]^\top \mapsto [ds_1, \dots, ds_n]^\top, \quad (52)$$

with the diagonal operator factor d obeying $d > 1$.

The following lemma shows that $\bar{\lambda}_{ij}$ in (48), which characterizes the dependency between the state errors of nodes i and j , satisfies the cyclic small-gain condition.

Lemma 12. Suppose Assumptions 1 and 3 hold, consider $\bar{\lambda}_{ij}$, η and ζ defined in (48), (35) and (45), respectively. If $1 < \eta < (1/\zeta)^{\frac{1}{\mathcal{D}(G)}}$, then there exists $d > 1$ such that

$$d\bar{\lambda}_{i_1 i_2} \times d\bar{\lambda}_{i_2 i_3} \times \dots \times d\bar{\lambda}_{i_r i_1} < 1 \quad (53)$$

for all $r \in \{1, \dots, n\}$ and $i_j \in \{1, \dots, n\}$, with $j \in \{1, \dots, r\}$ and $i_j \neq i_{j'}$ if $j \neq j'$. In particular, when $r = 1$, there holds $d\bar{\lambda}_{ii} < 1$ for all $i \in \{1, \dots, n\}$.

Lemma 12 leads to the existence of a vector of \mathcal{K}_∞

functions, $\sigma \in \mathcal{K}_\infty^n$, called a \mathcal{K} -path in [24], [25]. This allows for the construction of an ISS Lyapunov function for DBMC by scaling the Lyapunov-like functions of individual nodes, as obtained in Lemma 11, with the component of σ .

Furthermore, the subsequent theorem demonstrates that DBMC not only admits an ISS Lyapunov function but also an expISS one, as defined in Definition 7, owing to the linear dependence between the Lyapunov-like functions of the nodes, which ultimately establishes the expISS of DBMC.

Theorem 5. *Suppose Assumptions 1 and 3 hold, consider (35), with $e_i(t)$ the state error of node i , $u_{ij}(t)$, η and ζ defined in (37), (35) and (45), respectively. If $1 < \eta < (1/\zeta)^{\frac{1}{\mathcal{D}(G)}}$, then (35) admits an expISS Lyapunov function defined in Definition 7, using $e(t)$ the state error vector as the argument and $u(t) = (u_{ij})_{i \in V, j \in \mathcal{N}(i)}$ as the input.*

Proof. Given that (53) holds as Lemma 12 is applicable, it follows from Theorem 6.4 in [25] that there exists a diagonal operator D , as defined in (52), with the diagonal operator factor $d > 1$, and a vector of \mathcal{K}_∞ functions $\sigma = [\sigma_1, \dots, \sigma_n]^\top \in \mathcal{K}_\infty^n$, such that for all $s > 0$

$$D(\Gamma_{\oplus}(\sigma(s))) < \sigma(s),$$

where $\sigma(s) := [\sigma_1(s), \dots, \sigma_n(s)]^\top$ and Γ_{\oplus} is defined in (51). Combining this with the fact that $\bar{\lambda}_{ij}$ in Γ defined in (48) and the diagonal operator factor d of the diagonal operator D defined in (52) are both constants, it follows from [36] and Corollary 5.7 in [23] that σ in the above inequality can be a vector of linear \mathcal{K}_∞ functions.

Using σ as described above, as Γ is irreducible, it follows from Corollary 5.6 in [24] that for any $i \in \{1, \dots, n\}$, there exists a $\varphi \in \mathcal{K}_\infty$ such that for all $s > 0$,

$$\Gamma_{\oplus, i}(\sigma(s)) + \lambda_{iu}(\varphi(s)) < \sigma_i(s) \quad (54)$$

where $\Gamma_{\oplus, i}(\sigma(s))$ and $\sigma_i(s)$ in (54) are the i -th component of $\Gamma_{\oplus}(\sigma(s))$ and $\sigma(s)$, respectively, and λ_{iu} is defined in (47). Furthermore, as (50) holds, together with (54), it can be verified that the conditions in Theorem 5.3 of [24] are satisfied. By Theorem 5.3, the ISS Lyapunov function of (35) can be constructed as

$$V(e(t)) = \max_{i \in \{1, \dots, n\}} \sigma_i^{-1}(V_i(e_i(t))), \quad (55)$$

where σ_i^{-1} obeys $\sigma_i^{-1}(\sigma_i(s)) = s$ for all $s \geq 0$, and

$$V(e(t)) \geq \varphi^{-1}(\eta|u(t)|) \implies \dot{V}(e(t)) \leq \alpha(V(e(t))) \quad (56)$$

with α in (56) a positive definite function and $\varphi^{-1} \in \mathcal{K}_\infty$ obeying $\varphi^{-1}(\varphi(s)) = s$ for all $s \geq 0$.

Note that σ_i^{-1} is linear. As $V_i(\cdot) = |\cdot|$, $V(\cdot)$ defined in (55) satisfies (42) with $b = 1$. Further, as in (50) $\eta - 1 > 0$ is a constant and σ_i^{-1} is linear for $i \in \{1, \dots, n\}$, following the proof in Theorem 5.3 of [24], α in (56) can be chosen as a linear \mathcal{K}_∞ function, indicating that (43) also holds for $V(\cdot)$ defined in (55). Therefore, $V(\cdot)$ defined in (55) also serves as an implication-form expISS Lyapunov function for (35), which means that the nominal DBMC is expISS. ■

Remark 8. *In the proof of PPT and PT controls for DBMC, as well as in the small-gain based analysis, certain characteristics distinguishing directed and undirected graphs, such as the Laplacian matrix and symmetric neighbor relationship*

(i.e., $j \in \mathcal{N}(i)$ implies $i \in \mathcal{N}(j)$), have not been utilized. Consequently, the proposed control strategies and analyses can be extended to specific types of directed graphs, including directed strongly connected graphs, where a directed path exists between every pair of nodes, and connected rooted graphs, where each node has a directed path to a root node.

V. SIMULATIONS

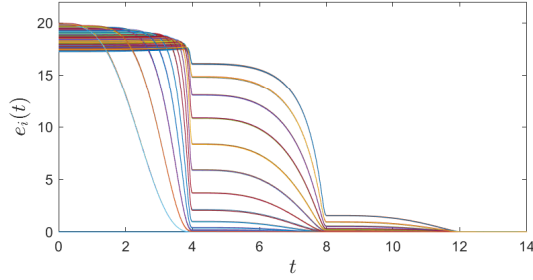
In this section, we empirically validate the theoretical results presented in the previous sections. Unless stated otherwise, all simulations are conducted on a 4×1 km² field with 500 nodes, including one source. All the nodes are randomly distributed and communicating within a range of 0.25 km.

A. The practical pre-specified finite time control strategy

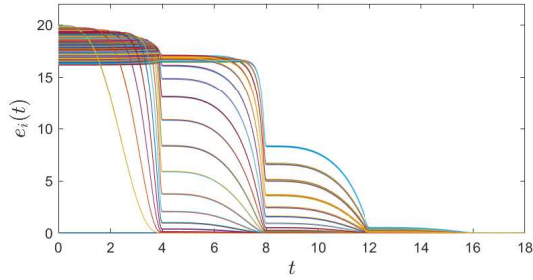
We first use the TBG $\varepsilon(t)$ defined in (7) to construct our TBG gain $\eta(t)$ as specified in (6). In this case $T_s = 4$. By setting δ in (6) to $\delta = 10^{-4}$, the simulation results are shown in Figure 3 (a) and (b). In this scenario, all initial states are set as overestimates such that Assumption 2 holds. In Figure 3 (a), the effective diameter $\mathcal{D}(G) = 20$, the state error $e_i(t)$ of each node $i \in V$ drops rapidly below the bound provided in Theorem 2 within $3 * T_s = 12$ units of time, which is less than the theoretical bound $(\mathcal{D}(G) - 1)T_s$ units of time. Similarly, in Figure 3, the state errors fall below the bound within $3 * T_s = 12$ units of time, while $\mathcal{D}(G)$ in this scenario is 22. A reasonable explanation could be that the greatest overestimate $V^+(t)$, i.e., the largest state error, is non-increasing itself by Lemma 2. Additionally, the graph structural aspects will also influence the time required to ensure all state errors are bounded. Figure 3 (c) and (d) illustrate that implementing the protocol on line graphs with 50 and 100 nodes (in both line graphs the source node is located at the rightmost end such that the number of nodes is equal to the effective diameter), requires significantly more time to bound the state errors compared to randomized graphs, despite having fewer nodes. For the line graph with 50 nodes, $10 * T_s = 40$ units of time is needed for the state errors to drop below the bound, whereas the line graph with 100 nodes requires $22 * T_s = 88$ units of time.

B. The pre-specified finite time control strategy

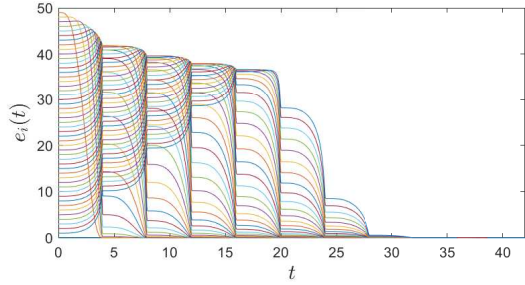
Next, we investigate the performance of the pre-specified finite time control strategy. In this scenario, we implement (25) on a randomized graph with $\mathcal{D}(G) = 21$, while setting all the initial states to be 20, which are overestimates. For $\bar{\eta}(t)$ defined in (26), we first fix $h = 12$ and $\gamma = 1$ while varying \bar{T}_s , which is the prescribed time for the convergence of DBMC. It has been shown in Figure 4 (a) and (b) that all state errors converge within the prescribed time of $\bar{T}_s = 2$ and $\bar{T}_s = 4$ units of time, respectively. Further, we fix $h = 12$ and $\bar{T}_s = 4$ while increasing γ from 1 to 10, i.e., increasing the feedback gain. The results are shown in Figure 4 (c). In this case, all state errors still converge within $\bar{T}_s = 4$ units of time. However, comparing Figure 4 (c) with Figure 4 (b), we can conclude that a larger γ leads to better convergence.



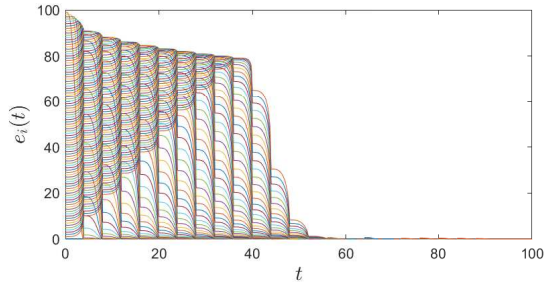
(a) Randomized graph with $\mathcal{D}(G) = 20$



(b) Randomized graph with $\mathcal{D}(G) = 22$

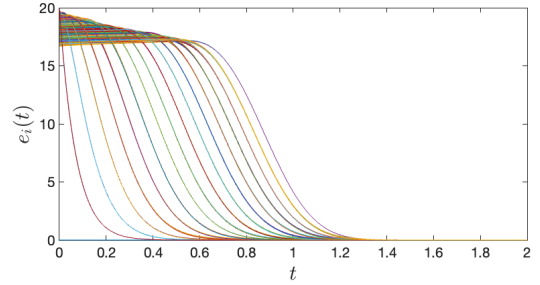


(c) Line graph with $n = \mathcal{D}(G) = 50$

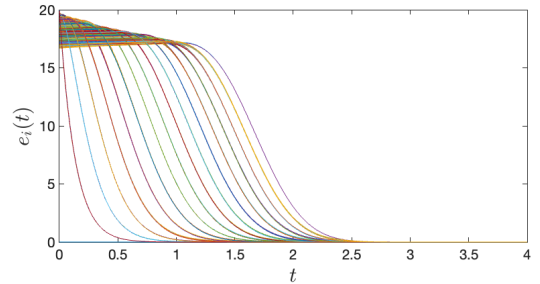


(d) Line graph with $n = \mathcal{D}(G) = 100$

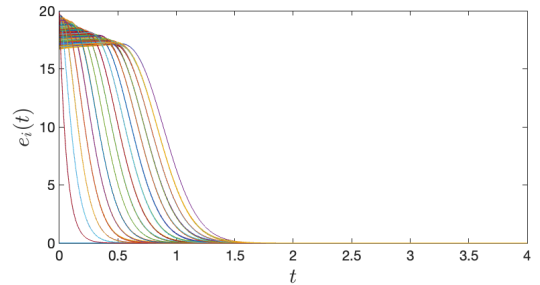
Fig. 3: Results of applying DBMC using the practical pre-specified finite time control strategy to both randomized graphs and line graphs. In all scenarios, state errors drop below the bound given in Theorem 2. It takes significantly longer time for line graphs than randomized graphs for the state errors to be bounded, while the time needed for all the cases are less than the theoretical bound given in Theorem 2.



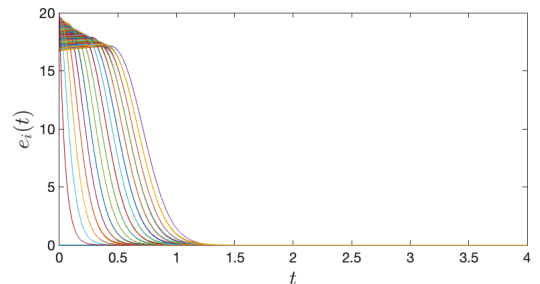
(a) Randomized graph with $\bar{T}_s = 2, h = 12, \gamma = 1$



(b) Randomized graph with $\bar{T}_s = 4, h = 12, \gamma = 1$



(c) Randomized graph with $\bar{T}_s = 4, h = 12, \gamma = 10$



(d) Randomized graph with $\bar{T}_s = 4, h = 20, \gamma = 10$

Fig. 4: Results of applying DBMC using the pre-specified finite time control strategy to randomized graphs. In all scenarios, the state errors converge to 0 within the prescribed time. The protocol achieves a better convergence effect with a larger h or γ .

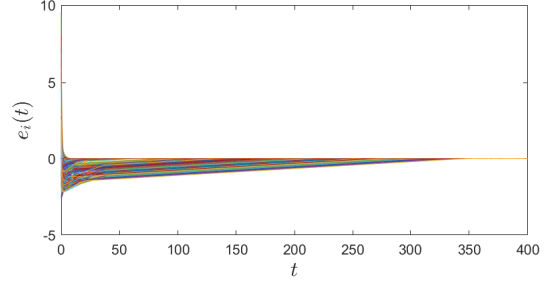
Specifically, at the same time instant, the state error with $\gamma = 10$ is much less than that with $\gamma = 1$. The same argument holds for cases with a larger h . In Figure 4 (d) we fix $\gamma = 10$ and $\bar{T}_s = 4$ while using $h = 20$, comparing this with Figure 4 (c), the convergence effect in this case is even better.

C. The nominal DBMC under perturbations

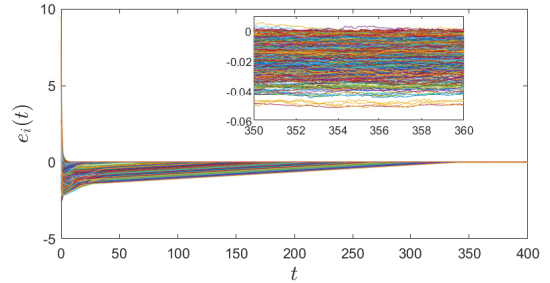
In this part, we examine the behaviors of DBMC under perturbations, including changes in the source set and the measurement noise on the edge weights. Unlike the previous two subsection, we do not impose the restriction that all states need to be overestimates. Instead, we assume all initial state are randomly distributed between $[0, 10]$, thus encompassing both overestimates and underestimates. We first set η in (3) as $\eta = 1 + 10^{-8}$, satisfying the condition on η in Theorem 5. Figure 5 (a) demonstrates the state errors with 0-input. In this scenario, DBMC converges exponentially fast, in accordance with the definition of expISS in Definition 6. Additionally, Figure 5 (a) shows that states starting with overestimates converge much faster than those with underestimates. Therefore, to achieve a better convergence speed, it is beneficial to set all initial states in the nominal DBMC to be overestimates. Figure 5 (b) further provides the trajectories of state errors under perturbations on the edge weights, assuming each edge weight $w_{ij}(t)$ varies continuously from $0.9w_{ij}$ to $1.1w_{ij}$. Similarly, all state errors drop below a bound at an exponential rate, with those starting as overestimates declining even faster. Notably, the largest state error is around 0.05, while $u_{ij}(t)$ defined in (37) obeys $u_{ij}(t) \leq 0.025$ for all $i \in V, j \in \mathcal{N}(i)$ and all $t \geq 0$, indicating the superior robustness of DBMC. Figure 5 further consolidates this claim. In this case, the edge weight $w_{ij}(t)$ varies from continuously $0.8w_{ij}$ to $1.2w_{ij}$ while $\eta = 1 + 10^{-8}$, the largest state error is now roughly 0.13, implying that it linearly depends on the magnitude of the input.

We next violate the condition in Theorem 5 by increasing η from $1 + 10^{-8}$ to 20, while $w_{ij}(t)$ still varies from $0.9w_{ij}$ to $1.1w_{ij}$ continuously. As shown in Figure 5 (c), (3) remains expISS, with all state errors dropping below the bound much more rapidly as the feedback gain increases. This shows the conservatism of the requirement on η in Theorem 5, stemming from the conservative nature of Lyapunov-based analysis.

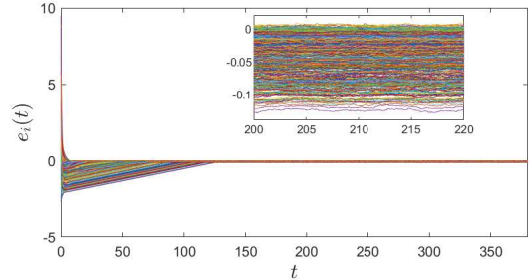
Finally, we consider the scenario where the source changes during the implementation of the nominal DBMC. In this scenario, $\eta = 1 + 10^{-8}$, the edge weights still bear the previous perturbation, and the source node changes from node 1 to node 20 when $t = 380$. As shown in Figure 6, initially, all state errors decline rapidly until they drop below the bound. Then abrupt spikes emerge at $t = 380$ as now the source changes to node 20. This leads to a discrepancy between the estimated distance to the previous source and the true distance from current source, creating new initial state errors. Since DBMC is globally exponentially input-to-state stable, i.e., all state errors will drop below a bound defined by the deviation of edge weight from its nominal value at an exponential rate regardless of the initial states, the state errors decline below the bound again after the source change.



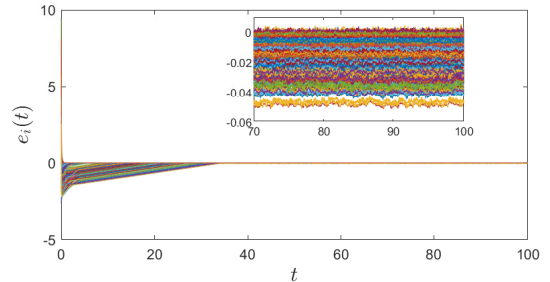
(a) DBMC without perturbations using $\eta = 1 + 10^{-8}$



(b) DBMC with $0.9w_{ij} \leq w_{ij}(t) \leq 1.1w_{ij}$ using $\eta = 1 + 10^{-8}$



(c) DBMC with $0.8w_{ij} \leq w_{ij}(t) \leq 1.2w_{ij}$ using $\eta = 1 + 10^{-8}$



(d) DBMC with $0.9w_{ij} \leq w_{ij}(t) \leq 1.1w_{ij}$ using $\eta = 20$

Fig. 5: Results of applying nominal DBMC to randomized graphs with varying η . With $\eta = 1 + 10^{-8}$, the nominal DBMC achieves exponential stability without perturbations and expISS with the edge weight $w_{ij}(t)$ ranging from $0.8w_{ij}$ to $1.2w_{ij}$. The nominal DBMC can still achieve expISS with a larger η , manifesting the conservatism of Lyapunov-based analysis.

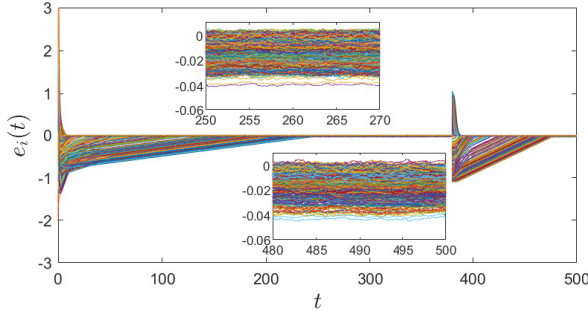
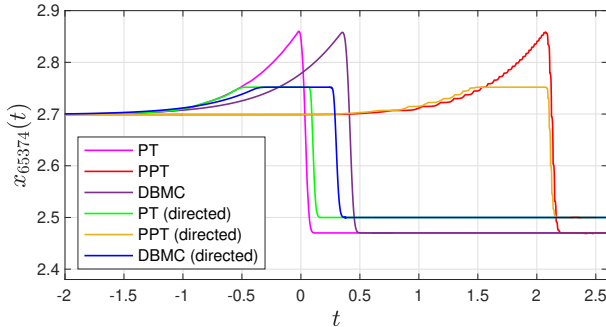


Fig. 6: Results of applying nominal DBMC to randomized graphs with the change of source. In this scenario, the source changes from node 1 to node 20 at $t = 380$ while $w_{ij}(t)$ ranges from $0.9w_{ij}$ to $1.1w_{ij}$ continuously. (3) is expISS before and after the source change.



(a) Shortest path calculation for robotic path planning



(b) Comparison of distance estimates using PT, PPT, and the nominal DBMC on directed and undirected grid graphs (both the x-axis and y-axis are plotted on a base-10 logarithmic scale.)

Fig. 7: Results of applying DBMC with PT and PPT control strategies, and the nominal DBMC to the shortest path calculation for robotic path planning on both undirected and directed grid graphs.

D. Application of DBMC in path planning

The simulation environment in this test employs a grid-based scanned map of a Parisian district from [37]. This 256×256 grid map designates black regions as building obstacles and white regions as traversable areas. To construct the path network, each grid point is treated as a network

node. Nodes in white regions have eight adjacent neighbors in the directions of up, down, left, right, upper-left, lower-left, upper-right, and lower-right, representing feasible movement directions for robotic agents. Conversely, nodes in black regions are isolated within the network, with no connections to any other nodes due to their untraversable nature. The resulting large-scale path network consists of 65,536 nodes and 354,938 edges, serving as the testbed for evaluating the proposed algorithm. The edge weight between each node and its adjacent nodes in the up, down, left, and right directions is 1, while the weight between each node and its diagonal neighbors in the upper-left, lower-left, upper-right, and lower-right directions is $\sqrt{2}$. In this simulation, we apply DBMC with PT and PPT control strategies, as well as the nominal DBMC, to the shortest path calculation for a robotic agent starting at its departure point, represented by a red square (node 65374) at the bottom of Figure 7 (a), and moving to its destination, represented by a red star at the top left corner (node 1) of the figure. Figure 7 (a) and (b) show that all three methods lead to the shortest path, represented by the red line in Figure 7 (a). Figure 7 (b) further demonstrates that DBMC with PT control strategy achieves the fastest convergence speed within the pre-specified 4 units of time, followed by the nominal DBMC with the use of a high feedback gain $\eta = 100$, and DBMC with PPT control strategy, which exhibits the slowest convergence, stabilizing within $\mathcal{D}(G) - 1$ times the pre-specified 4 units of time, as established in Theorem 2.

We next empirically evaluate the efficacy of DBMC on directed graphs. For the nodes in white regions within the grey rectangle of Figure 7 (a), the number of neighbors is reduced from eight to three, retaining only those in the directions of right, upper-right, and lower-right, thus transforming the undirected graph into a directed one. With this modification, we continue to apply DBMC with PT and PPT control strategies, as well as the nominal DBMC, to compute the shortest path for a robotic agent from node 65374 to node 1. As shown in Figure 7 (a), all three methods result in the same shortest path, represented by the blue line, which circumvents the original path due to the grey rectangle zone. Figure 7 (b) further shows that the convergence patterns of these three methods remain consistent with those observed on the undirected graph.

VI. CONCLUSIONS

In this paper, both PPT and PT control strategies have been designed for DBMC. Under the proposed control strategies, DBMC can converge to the stationary value exactly or to a certain level adjustable by a user-defined parameter, within a prescribed finite time without dependence on the initial states. Regarding the nominal DBMC, we have provided the sufficient condition for the range of the feedback gain to ensure its expISS, i.e., DBMC is globally exponentially stable without perturbations, and with perturbations, its state error will drop exponentially fast below a bound defined by the magnitude of the perturbation. An interesting research direction would be designing a second or higher order DBMC, as many systems in engineering are modeled by higher order dynamics, and several works on higher-order min-consensus protocols [38]

are worthy of reference. It is also important to note that for some general directed graphs, such as weakly connected ones where some nodes lack a directed path to the source, DBMC may cause disconnected nodes to retain their initial states. Additionally, nodes with a directed path to the source that also connect to these disconnected nodes may be influenced by them, hindering the attainment of the shortest path. Another interesting direction for future work would be to enhance DBMC in such scenarios, ensuring that nodes with a directed path to the source can obtain the shortest path.

REFERENCES

- [1] D. Yao, H. Li, and Y. Shi, "Event-based average consensus of disturbed mass via fully distributed sliding mode control," *IEEE Transactions on Automatic Control*, 2023.
- [2] V. Yadav and M. Salapaka, "Distributed protocol for determining when averaging consensus is reached," in *45th Annual Allerton Conference on Communication, Control, and Computing*, 2007, pp. 715–720.
- [3] J. Cortés, "Distributed algorithms for reaching consensus on general functions," *Automatica*, vol. 44, no. 3, pp. 726–737, 2008.
- [4] Y. Zhang and S. Li, "Distributed biased min-consensus with applications to shortest path planning," *IEEE Transactions on Automatic Control*, vol. 62, no. 10, pp. 5429–5436, Oct 2017.
- [5] R. Bellman, "On a routing problem," *Quarterly of applied mathematics*, vol. 16, no. 1, pp. 87–90, 1958.
- [6] E. W. Dijkstra, "A note on two problems in connexion with graphs," in *Edsger Wybe Dijkstra: His Life, Work, and Legacy*, 2022, pp. 287–290.
- [7] S. J. Russell and P. Norvig, *Artificial intelligence: a modern approach*. Pearson, 2016.
- [8] X. Shi, Y. Xu, and H. Sun, "A biased min-consensus-based approach for optimal power transaction in multi-energy-router systems," *IEEE Transactions on Sustainable Energy*, vol. 11, no. 1, pp. 217–228, 2018.
- [9] Y. Zhang and S. Li, "Perturbing consensus for complexity: A finite-time discrete biased min-consensus under time-delay and asynchronism," *Automatica*, vol. 85, pp. 441–447, 2017.
- [10] P. Yao, R. Zhao, and Q. Zhu, "A hierarchical architecture using biased min-consensus for USV path planning," *IEEE Transactions on Vehicular Technology*, vol. 69, no. 9, pp. 9518–9527, 2020.
- [11] X. Shi, Y. Xu, Q. Guo *et al.*, "A distributed EV navigation strategy considering the interaction between power system and traffic network," *IEEE Transactions on Smart Grid*, vol. 11, no. 4, pp. 3545–3557, 2020.
- [12] Y. Mo, S. Dasgupta, and J. Beal, "Robustness of the adaptive Bellman-Ford algorithm: Global stability and ultimate bounds," *IEEE Transactions on Automatic Control*, pp. 4121–4136, 2019.
- [13] Y. Mo, S. Dasgupta, and J. Beal, "Stability and resilience of distributed information spreading in aggregate computing," *IEEE Transactions on Automatic Control*, vol. 68, no. 1, pp. 454–461, 2022.
- [14] Y. Mo and L. Yu, "A Lyapunov analysis of the continuous-time adaptive Bellman-Ford algorithm," *Systems & Control Letters*, vol. 157, p. 105045, 2021.
- [15] A. Paulos, S. Dasgupta, J. Beal *et al.*, "A framework for self-adaptive dispersal of computing services," in *2019 IEEE 4th International Workshops on Foundations and Applications of Self* Systems (FAS* W)*. IEEE, 2019, pp. 98–103.
- [16] Y. Song, H. Ye, and F. L. Lewis, "Prescribed-time control and its latest developments," *IEEE Transactions on Systems, Man, and Cybernetics: Systems*, 2023.
- [17] B. Ning, Q.-L. Han, Z. Zuo *et al.*, "Fixed-time and prescribed-time consensus control of multiagent systems and its applications: A survey of recent trends and methodologies," *IEEE Transactions on Industrial Informatics*, vol. 19, no. 2, pp. 1121–1135, 2022.
- [18] Y. Wang and Y. Song, "Leader-following control of high-order multi-agent systems under directed graphs: Pre-specified finite time approach," *Automatica*, vol. 87, pp. 113–120, 2018.
- [19] Y. Wang, Y. Song, D. J. Hill *et al.*, "Prescribed-time consensus and containment control of networked multiagent systems," *IEEE Transactions on Cybernetics*, vol. 49, no. 4, pp. 1138–1147, 2018.
- [20] P. Krishnamurthy, F. Khorrarni, and M. Krstic, "A dynamic high-gain design for prescribed-time regulation of nonlinear systems," *Automatica*, vol. 115, p. 108860, 2020.
- [21] Y. Cao, J. Cao, and Y. Song, "Practical prescribed time tracking control over infinite time interval involving mismatched uncertainties and non-vanishing disturbances," *Automatica*, vol. 136, p. 110050, 2022.
- [22] B. Ning, Q.-L. Han, and Z. Zuo, "Practical fixed-time consensus for integrator-type multi-agent systems: A time base generator approach," *Automatica*, vol. 105, pp. 406–414, 2019.
- [23] R. Geiselhart and F. R. Wirth, "Relaxed ISS small-gain theorems for discrete-time systems," *SIAM Journal on Control and Optimization*, vol. 54, no. 2, pp. 423–449, 2016.
- [24] S. N. Dashkovskiy, B. S. Rüffer, and F. R. Wirth, "Small gain theorems for large scale systems and construction of ISS Lyapunov functions," *SIAM Journal on Control and Optimization*, vol. 48, no. 6, pp. 4089–4118, 2010.
- [25] B. S. Rüffer, "Monotone inequalities, dynamical systems, and paths in the positive orthant of Euclidean n-space," *Positivity*, vol. 14, pp. 257–283, 2010.
- [26] X. Gong, Y. Cui, J. Shen *et al.*, "Distributed optimization in prescribed-time: Theory and experiment," *IEEE Transactions on Network Science and Engineering*, vol. 9, no. 2, pp. 564–576, 2021.
- [27] Y. Zheng, Q. Liu, and J. Wang, "A specified-time convergent multi-agent system for distributed optimization with a time-varying objective function," *IEEE Transactions on Automatic Control*, vol. 69, no. 2, pp. 1257–1264, 2023.
- [28] I. Daanoun, B. Abdennaceur, and A. Ballouk, "A comprehensive survey on leach-based clustering routing protocols in wireless sensor networks," *Ad Hoc Networks*, vol. 114, p. 102409, 2021.
- [29] H. K. Khalil, "Nonlinear systems," *Upper Saddle River*, 2002.
- [30] P. Morasso, V. Sanguineti, and G. Spada, "A computational theory of targeting movements based on force fields and topology representing networks," *Neurocomputing*, vol. 15, no. 3-4, pp. 411–434, 1997.
- [31] F. H. Clarke, *Optimization and Nonsmooth Analysis*. SIAM, 1990.
- [32] J. Stewart, *Multivariable Calculus: Early Transcendentals*. Cengage Learning, 2007.
- [33] W. M. Haddad and V. Chellaboina, *Nonlinear dynamical systems and control: a Lyapunov-based approach*. Princeton university press, 2008.
- [34] A. Mironchenko, *Input-to-State Stability*. Cham: Springer International Publishing, 2023, pp. 41–115.
- [35] A. Berman and R. J. Plemmons, *Nonnegative matrices in the mathematical sciences*. SIAM, 1994.
- [36] R. Geiselhart and F. Wirth, "Numerical construction of LISS Lyapunov functions under a small-gain condition," *Mathematics of Control, Signals, and Systems*, vol. 24, pp. 3–32, 2012.
- [37] R. Stern, N. Sturtevant, A. Felner *et al.*, "Multi-agent pathfinding: Definitions, variants, and benchmarks," in *Proceedings of the International Symposium on Combinatorial Search*, vol. 10, no. 1, 2019, pp. 151–158.
- [38] B. Singh, A. Sen, and S. R. Sahoo, "Min-consensus for heterogeneous higher-order integrators under switching digraph," *IEEE Control Systems Letters*, vol. 4, no. 3, pp. 560–565, 2020.

APPENDIX

Proof of Theorem 1: It follows from Remark 3 that $0 \leq \eta(t) \leq L$ for all $t \geq 0$ with some $L > 0$. For $i \in V$, define a nonlinear map $f_i : [0, +\infty) \times \mathbb{R}^n \rightarrow \mathbb{R}$ such that $f_i(t, \tilde{x}) = 0$ for $i \in S$ and $f_i(t, \tilde{x}) = -\eta(t)(\tilde{x}_i - \min_{j \in \mathcal{N}(i)} \{\tilde{x}_j + w_{ij}\})$ for $i \in V \setminus S$, with $\tilde{x} = [\tilde{x}_1, \dots, \tilde{x}_n]^\top \in \mathbb{R}^n$ and $i \in \{1, \dots, n\}$. The composite map is defined as $f : [0, +\infty) \times \mathbb{R}^n \rightarrow \mathbb{R}^n$. Then for any $\bar{x} = [\bar{x}_1, \dots, \bar{x}_n]^\top \in \mathbb{R}^n$, there holds

$$|f(t, \tilde{x}) - f(t, \bar{x})|_\infty = |f_i(t, \tilde{x}) - f_i(t, \bar{x})| \quad (57)$$

$$\leq L|\tilde{x}_i - \bar{x}_i| + L \left| \min_{j \in \mathcal{N}(i)} \{\tilde{x}_j + w_{ij}\} - \min_{j \in \mathcal{N}(i)} \{\bar{x}_j + w_{ij}\} \right|$$

$$\leq L|\tilde{x}_i - \bar{x}_i| + L|\tilde{x}_{i'} + w_{ii'} - (\bar{x}_{i'} + w_{ii'})| \quad (58)$$

$$\leq L|\tilde{x}_i - \bar{x}_i| + L|\tilde{x}_{j'} + w_{ij'} - (\bar{x}_{j'} + w_{ij'})| \quad (59)$$

$$\leq 2L|\tilde{x} - \bar{x}|_\infty$$

where in (57) we assume $i = \arg \max_{j \in \{1, \dots, n\}} \{f_j(t, \tilde{x}) - f_j(t, \bar{x})\}$, in (58) we assume $i' = \arg \min_{j \in \mathcal{N}(i)} \{\tilde{x}_j + w_{ij}\}$ and $j' = \arg \min_{j \in \mathcal{N}(i)} \{\bar{x}_j + w_{ij}\}$, and (59) uses the fact that $\tilde{x}_{i'} + w_{ii'} \leq \bar{x}_j + w_{ij}$ for all $j \in \mathcal{N}(i)$ and $j' \in \mathcal{N}(i)$ (in (59) we also assume without loss of generality that $\tilde{x}_{i'} + w_{ii'} > \tilde{x}_{j'} + w_{ij'}$). Therefore, the composite map $f(\cdot, \cdot)$ is globally Lipschitz continuous with respect to its second argument for

$t \geq 0$ and continuous with respect to its first argument, from Theorem 3.2 in [29], (5) admits a unique solution.

Proof of Lemma 1: It can be readily verified that the solution to (8) over the interval $[0, T_s]$ obeys

$$y(t) = y_0 \left(1 - \frac{\varepsilon(t)}{1 + \delta}\right), \quad (60)$$

and thus we have $y(T_s) = \frac{\delta}{1 + \delta} y(0)$.

Proof of Lemma 5: We prove our claim by induction. We begin with $\ell = 1$, for $i \in \mathcal{F}_1$, it has a true parent node $j \in S = \mathcal{F}_0$, then it follows from (5) and (9) that for all $t \in [0, T_s]$

$$\begin{aligned} \dot{e}_i(t) &= \dot{x}_i(t) = -\eta(t)(x_i(t) - \min_{k \in \mathcal{N}(i)} \{x_k(t) + w_{ik}\}) \\ &= -\eta(t)(x_i(t) - (x_j^* + w_{ij})) \end{aligned} \quad (61)$$

$$= -\eta(t)e_i(t) \quad (62)$$

where (61) uses the following four aspects: 1) $x_i(t) \geq x_i^*$ for $t \geq 0$ and all $i \in V$ by Lemma 4; 2) $x_i(t) = 0 = x_i^*$ for $t \geq 0$ and all $i \in \mathcal{F}_0 = S$; 3) $j \in S$ is the true parent node of i ; and 4) the stationary value defined by (1), and thus $x_j(t) + w_{ij} = x_j^* + w_{ij} \leq \min_{k \in \mathcal{N}(i)} \{x_k^* + w_{ik}\} \leq \min_{k \in \mathcal{N}(i)} \{x_k(t) + w_{ik}\}$, and (62) uses (1). Further, by Lemma 1, for $t \in [0, T_s]$

$$e_i(t) = e_i(0) \left(1 - \frac{\varepsilon(t)}{1 + \delta}\right) \leq e_{\max}(0) \left(1 - \frac{\varepsilon(t)}{1 + \delta}\right), \quad (63)$$

and thus $e_i(T_s) \leq \frac{\delta}{1 + \delta} e_{\max}(0)$.

We next prove that $e_i(t) \leq e_i(T_s)$ for all $t \geq T_s$. Note that $\dot{e}_i(t) = -\eta(t)e_i(t)$ still holds for $t \geq T_s$. Applying Lemma 1 on $\dot{e}_i(t)$ over the interval $[T_s, 2T_s]$, we obtain

$$e_i(t) = e_i(T_s) \left(1 - \frac{\varepsilon(t - T_s)}{1 + \delta}\right) \leq e_i(T_s), \forall t \in [T_s, 2T_s]. \quad (64)$$

Repeating the above procedure, it holds that $e_i(t) \leq e_i(T_s) = \frac{\delta}{1 + \delta} e_{\max}(0)$ for all $t \geq T_s$, and (23) holds with $\ell = 1$.

Suppose (23) holds with some $\ell \in \{1, \dots, \mathcal{D}(G) - 2\}$. For $i \in \mathcal{F}_{\ell+1}$, from (5) and (9), we have $\forall t \in [\ell T_s, (\ell + 1)T_s]$,

$$\begin{aligned} \dot{e}_i(t) &= \dot{x}_i(t) = -\eta(t)(x_i(t) - \min_{k \in \mathcal{N}(i)} \{x_k(t) + w_{ik}\}) \\ &\leq -\eta(t)(x_i(t) - (x_j(t) + w_{ij})) \end{aligned} \quad (65)$$

$$\begin{aligned} &= -\eta(t)(x_i^* + e_i(t) - (x_j^* + e_j(t) + w_{ij})) \\ &\leq -\eta(t)(e_i(t) - \frac{\ell\delta}{1 + \delta} e_{\max}(0)) \end{aligned} \quad (66)$$

where in (65) we assume $j \in \mathcal{P}(i)$, and (66) uses (1), the fact that $j \in \mathcal{F}_\ell$ and our induction hypothesis that $e_j(t) \leq \frac{\ell\delta}{1 + \delta} e_{\max}(0)$ for all $t \geq \ell T_s$.

As (66) implies $(e_i(t) - \ell \frac{\delta}{1 + \delta} e_{\max}(0))' \leq -\eta(t)(e_i(t) - \ell \frac{\delta}{1 + \delta} e_{\max}(0))$, by applying Lemma 1 and comparison principle [29], we obtain for $t \in [\ell T_s, (\ell + 1)T_s]$

$$\begin{aligned} e_i(t) - \ell \frac{\delta}{1 + \delta} e_{\max}(0) &\leq (e_i(\ell T_s) - \ell \frac{\delta}{1 + \delta} e_{\max}(0)) \left(1 - \frac{\varepsilon(t - \ell T_s)}{1 + \delta}\right), \end{aligned} \quad (67)$$

which further leads to

$$\begin{aligned} e_i((\ell + 1)T_s) &\leq (e_{\max}(0) - \frac{\ell\delta}{1 + \delta} e_{\max}(0)) \frac{\delta}{1 + \delta} + \frac{\ell\delta}{1 + \delta} e_{\max}(0) \\ &\leq \frac{(\ell + 1)\delta}{1 + \delta} e_{\max}(0) \end{aligned} \quad (68)$$

where (68) uses Lemma 2 and $\varepsilon(T_s) = 1$. To complete our proof, we need to show that $e_i(t) \leq e_i((\ell + 1)T_s)$ for all $t \geq$

$(\ell + 1)T_s$. Again, note that (66) still holds over $[(\ell + 1)T_s, (\ell + 2)T_s]$, it follows from (67) that for $t \in [(\ell + 1)T_s, (\ell + 2)T_s]$

$$\begin{aligned} e_i(t) - \ell \frac{\delta}{1 + \delta} e_{\max}(0) &\leq (e_i((\ell + 1)T_s) - \frac{\ell\delta}{1 + \delta} e_{\max}(0)) \left(1 - \frac{\varepsilon(t - (\ell + 1)T_s)}{1 + \delta}\right) \\ &\leq e_i((\ell + 1)T_s) - \frac{\ell\delta}{1 + \delta} e_{\max}(0) \end{aligned} \quad (69)$$

where (69) uses the fact that $\varepsilon(t) \in [0, 1]$ for $t \in [0, T_s]$. Thus, repeating the same arguments iteratively for subsequent intervals, we can conclude that $e_i(t) \leq \frac{(\ell + 1)\delta}{1 + \delta} e_{\max}(0)$ for $t \geq (\ell + 1)T_s$, proving our claim.

Proof of Lemma 6: Multiplying $\rho^\alpha(t)$ on both sides of (28), we obtain

$$\rho^\alpha(t) \dot{y}(t) = -\gamma \rho^\alpha(t) y(t) - \alpha \rho(t)^{\alpha-1} \dot{\rho}(t) y(t) \quad (70)$$

which further gives

$$\frac{d(\rho^\alpha(t) y(t))}{dt} = \rho^\alpha(t) \dot{y}(t) + \alpha \rho(t)^{\alpha-1} \dot{\rho}(t) y(t) = -\gamma \rho^\alpha(t) y(t).$$

Applying comparison principle on the above equation gives

$$\rho^\alpha(t) y(t) = e^{-\gamma(t-t_0)} \rho^\alpha(t_0) y(t_0), \forall t \in [t_0, \bar{T}_s], \quad (71)$$

thus our claim follows.

Proof of Lemma 8: Consider a sequence of nodes i_0, i_1, \dots, i_T such that $i_\ell \in \mathcal{F}_\ell$ with $\ell \in \{0, \dots, T\}$ and i_ℓ is the true parent node of $i_{\ell+1}$ with $\ell \in \{0, \dots, T-1\}$. Every node in the graph G is in such a sequence and $T \leq \mathcal{D}(G) - 1$. As $\mathcal{F}_0 = S$ by Remark 1, we begin with node i_1 . It follows from (25) and (9) that for $t \in [0, \bar{T}_s]$

$$\begin{aligned} \dot{e}_{i_1}(t) &= \dot{x}_{i_1}(t) = -\bar{\eta}(t)(x_{i_1}(t) - \min_{j \in \mathcal{N}(i_1)} \{x_j(t) + w_{i_1 j}\}) \\ &= -\bar{\eta}(t)(x_{i_1}(t) - (x_{i_0}^* + w_{i_0 i_1})) \end{aligned} \quad (72)$$

$$= -\bar{\eta}(t)e_{i_1}(t) \quad (73)$$

where (72) uses Lemma 7 stating that $x_i(t) \geq x_i^*$ for all $i \in V$ and all $t \geq 0$, and the fact that $i_0 \in S$ is a true parent node of i_1 , i.e., for all $j \in \mathcal{N}(i_1)$, $x_{i_0}(t) + w_{i_0 i_1} = x_{i_0}^* + w_{i_0 i_1} = x_{i_1}^* \leq x_j^* + w_{i_1 j} \leq x_j(t) + w_{i_1 j}$, and (73) uses (1) and (9). From Lemma 6, (73) gives

$$e_{i_1}(t) = \rho^{-2}(t) e^{-\gamma t} e_{i_1}(0), \quad (74)$$

leading to $\lim_{t \rightarrow \bar{T}_s^-} e_{i_1}(t) = 0$, and $\lim_{t \rightarrow \bar{T}_s^-} x_{i_1}(t) = x_{i_1}^*$.

For node i_2 , we prove by contradiction. Suppose $e_{i_2}(t)$ does not converge to 0 when t approaches \bar{T}_s^- . As $e_i(t) \geq 0$ for all $i \in V$ and $t \in [0, \bar{T}_s)$ by Lemma 7, $\lim_{t \rightarrow \bar{T}_s^-} e_{i_2}(t) \neq 0$ is equivalent to $\exists \epsilon_1 > 0$, such that $\forall \delta_1 > 0$, there exists a $t_1 \in [\bar{T}_s - \delta_1, \bar{T}_s)$ such that $e_{i_2}(t_1) \geq \epsilon_1$. As $\lim_{t \rightarrow \bar{T}_s^-} e_{i_1}(t) = 0$ implies that for some $\epsilon_2 = \frac{1}{3}\epsilon_1$, $\exists \delta_2 > 0$ such that $e_{i_1}(t) < \epsilon_2$ for all $t \in [\bar{T}_s - \delta_2, \bar{T}_s)$, from (25) and (9), for $t \in [\bar{T}_s - \delta_2, \bar{T}_s)$

$$\begin{aligned} \dot{e}_{i_2}(t) &= -\bar{\eta}(t)(x_{i_2}(t) - \min_{j \in \mathcal{N}(i_2)} \{x_j(t) + w_{i_2 j}\}) \\ &\leq -\bar{\eta}(t)(x_{i_2}(t) - (x_{i_1}(t) + w_{i_1 i_2})) \\ &< -\bar{\eta}(t)(x_{i_2}(t) - (x_{i_1}^* + \epsilon_2 + w_{i_1 i_2})) \\ &= -\bar{\eta}(t)(e_{i_2}(t) - \epsilon_2) \end{aligned} \quad (75)$$

where (75) uses (1). Using comparison principle and Lemma 6, there holds for $t \in [\bar{T}_s - \delta_2, \bar{T}_s)$

$$e_{i_2}(t) \leq \underbrace{\rho^{-2}(t) \rho^2(\bar{T}_s - \delta_2) e^{-\gamma(t - (\bar{T}_s - \delta_2))}}_{\Delta(t)} (e_{i_2}(\bar{T}_s - \delta_2) - \epsilon_2) + \epsilon_2. \quad (76)$$

As the left-hand limit at \bar{T}_s of $\Delta(t)$ in (76) is 0, for $\epsilon_2 > 0$, $\exists \delta_3 > 0$ (such δ_3 can be chosen to satisfy $\delta_3 < \delta_2$) such that $|\Delta(t)| < \epsilon_2$ for all $t \in [\bar{T}_s - \delta_3, \bar{T}_s)$, leading to $e_{i_2}(t) \leq 2\epsilon_2 = \frac{2}{3}\epsilon_1$ for all $t \in [\bar{T}_s - \delta_3, \bar{T}_s)$, establishing the contradiction, and thus $\lim_{t \rightarrow \bar{T}_s^-} x_{i_2}(t) = x_{i_2}^*$.

To prove $\lim_{t \rightarrow \bar{T}_s^-} x_{i_2}(t) = x_{i_2}^*$, we only need to use the fact that $\lim_{t \rightarrow \bar{T}_s^-} x_{i_1}(t) = x_{i_1}^*$. By applying the same steps to the remaining nodes, it can be verified that $\lim_{t \rightarrow \bar{T}_s^-} x_{i_\ell}(t) = x_{i_\ell}^*$ for all $\ell \in \{1, \dots, T\}$, thus completing our proof.

Proof of Lemma 9: We use the sequence of nodes i_0, i_1, \dots, i_T as considered in the proof of Lemma 8. We begin with node $i_1 \in \mathcal{F}_1$, it follows from (73) and (74) in the proof of Lemma 8 that for $t \in [0, \bar{T}_s)$

$$\begin{aligned} \dot{e}_{i_1}(t) &= -\bar{\eta}(t)\rho^{-2}(t)e^{-\gamma t}e_{i_1}(0) \\ &= -\left(\gamma \frac{(\bar{T}_s - t)^{2+2h}}{\bar{T}_s^{2+2h}} + 2 \frac{(1+h)(\bar{T}_s - t)^{1+2h}}{\bar{T}_s^{2+2h}}\right)e^{-\gamma t}e_{i_1}(0), \end{aligned}$$

implying $\lim_{t \rightarrow \bar{T}_s^-} \dot{x}_{i_1}(t) = \dot{e}_{i_1}(t) = 0$. Further, we prove (32) by using induction and begin with node $i_2 \in \mathcal{F}_2$. It follows from (25) that over the interval $[0, \bar{T}_s)$:

$$\begin{aligned} \dot{e}_{i_2}(t) &= -\bar{\eta}(t) \left(x_{i_2}(t) - \min_{j \in \mathcal{N}(i_2)} \{x_j(t) + w_{ij}\} \right) \\ &\leq -\bar{\eta}(t)(x_{i_2}(t) - (x_{i_1}(t) + w_{i_1 i_2})) \end{aligned} \quad (77)$$

$$\begin{aligned} &= -\bar{\eta}(t)(x_{i_2}^* + e_{i_2}(t) - x_{i_1}^* - e_{i_1}(t) - w_{i_1 i_2}) \\ &= -\bar{\eta}(t)(e_{i_2}(t) - e_{i_1}(t)) \end{aligned} \quad (78)$$

where (77) uses $\bar{\eta}(t) > 0$ for $t \in [0, \bar{T}_s)$ and the fact that i_1 is a true parent node of i_2 and thus $i_1 \in \mathcal{N}(i_2)$, and (78) uses (1). Putting (74) and (26) into (77), there holds:

$$\begin{aligned} \dot{e}_{i_2}(t) &\leq \\ &\left(\gamma + \frac{2h+2}{\bar{T}_s - t}\right) \left(\frac{\bar{T}_s - t}{\bar{T}_s}\right)^{2h+2} e^{-\gamma t} e_{i_1}(0) - \left(\gamma + \frac{2h+2}{\bar{T}_s - t}\right) e_{i_2}(t) \\ &\leq \left(\gamma + \frac{2h+2}{\bar{T}_s - t}\right) \left(\frac{\bar{T}_s - t}{\bar{T}_s}\right)^{2h+2} e_{i_1}(0) - \left(\gamma + \frac{2h+1}{\bar{T}_s - t}\right) e_{i_2}(t) \quad (79) \\ &\leq C_{i_2} (\bar{T}_s - t)^{2h+1} - \left(\gamma + \frac{2h+1}{\bar{T}_s - t}\right) e_{i_2}(t) \end{aligned} \quad (80)$$

where (79) uses the fact that $e_{i_1}(t), e_{i_2}(t) \geq 0$ for $t \in [0, \bar{T}_s)$ by Lemma 7 and $0 < e^{-\gamma t} \leq 1$ for $t \in [0, \bar{T}_s)$, (80) follows that $0 < \frac{\bar{T}_s - t}{\bar{T}_s} \leq 1$ for $t \in [0, \bar{T}_s)$, and in (80) $C_{i_2} = \left(\frac{\gamma}{\bar{T}_s^{2h+1}} + \frac{2h+2}{\bar{T}_s^{2h+2}}\right) e_{i_1}(0)$. From (80), by the comparison principle, $e_{i_2}(t)$ is bounded above by the solution to the differential equation $\dot{\bar{e}}_{i_2}(t) = C_{i_2} (\bar{T}_s - t)^{2h+1} - \left(\gamma + \frac{2h+1}{\bar{T}_s - t}\right) \bar{e}_{i_2}(t)$ with the initial condition $\bar{e}_{i_2}(0) = e_{i_2}(0)$ for $t \in [0, \bar{T}_s)$. Therefore,

$$e_{i_2}(t) \leq \left(\frac{\bar{T}_s - t}{\bar{T}_s}\right)^{2h+1} (e^{-\gamma t} e_{i_2}(0) + c_{i_2}) \quad (81)$$

with $c_{i_2} = \frac{\bar{T}_s^{2h+1} C_{i_2}}{\gamma}$, and thus (32) holds for $\ell = 2$.

Suppose (32) holds for some $\ell \in \{2, \dots, \mathcal{D}(G) - 2\}$. For node $i_{\ell+1} \in \mathcal{F}_{\ell+1}$, from (25), (77) and (78), for $t \in [0, \bar{T}_s)$

$$\begin{aligned} \dot{e}_{i_{\ell+1}}(t) &\leq -\bar{\eta}(t)(e_{i_{\ell+1}}(t) - e_{i_\ell}(t)) \quad (82) \\ &\leq \left(\gamma + \frac{2h+2}{\bar{T}_s - t}\right) \left(\frac{\bar{T}_s - t}{\bar{T}_s}\right)^{2h+3-\ell} (e^{-\gamma t} e_{i_\ell}(0) + c_{i_\ell}) - \\ &\quad \left(\gamma + \frac{2h+2}{\bar{T}_s - t}\right) e_{i_{\ell+1}}(t) \end{aligned} \quad (83)$$

$$\leq C_{i_{\ell+1}} (\bar{T}_s - t)^{2h+2-\ell} - \left(\gamma + \frac{2h+2-\ell}{\bar{T}_s - t}\right) e_{i_{\ell+1}}(t) \quad (84)$$

where in (82) node $i_\ell \in \mathcal{F}_\ell$ is a true parent node of node $i_{\ell+1}$,

(83) uses our induction hypothesis that (32) holds for node i_ℓ , (84) uses the fact that $e_{i_{\ell+1}}(t) \geq 0$ for $t \in [0, \bar{T}_s)$ by Lemma 7, and in (84) $C_{i_{\ell+1}} = \left(\frac{\gamma}{\bar{T}_s^{2h+2-\ell}} + \frac{2h+2}{\bar{T}_s^{2h+3-\ell}}\right) (e_{i_\ell}(0) + c_{i_\ell})$. Following the derivation from (80) to (81), it follows from (84) that $e_{i_{\ell+1}}(t)$ obeys

$$e_{i_{\ell+1}}(t) \leq \left(\frac{\bar{T}_s - t}{\bar{T}_s}\right)^{2h+2-\ell} (e^{-\gamma t} e_{i_{\ell+1}}(0) + c_{i_{\ell+1}}) \quad (85)$$

with $c_{i_{\ell+1}} = \frac{\bar{T}_s^{2h+2-\ell} C_{i_{\ell+1}}}{\gamma}$. Therefore, our claim (32) follows.

Proof of Lemma 10: It follows from (25) that for $i \in \mathcal{F}_\ell$ with $\ell \in \{2, \dots, \mathcal{D}(G) - 1\}$

$$\begin{aligned} \dot{x}_i(t) &= \dot{e}_i(t) = -\eta(t)(x_i(t) - \min_{j \in \mathcal{N}(i)} \{x_j(t) + w_{ij}\}) \\ &\geq -\bar{\eta}(t)(x_i(t) - x_i^*) = -\bar{\eta}(t)e_i(t) \end{aligned} \quad (86)$$

where the inequality in (86) uses Lemma 7 and (1), resulting in $\min_{j \in \mathcal{N}(i)} \{x_j(t) + w_{ij}\} \geq \min_{j \in \mathcal{N}(i)} \{x_j^* + w_{ij}\} = x_i^*$. Putting (32) into (86) yields

$$\begin{aligned} \dot{e}_i(t) &\geq -\bar{\eta}(t) \frac{(\bar{T}_s - t)^{2h+3-\ell}}{\bar{T}_s^{2h+3-\ell}} (e^{-\gamma t} e_i(0) + c_i) \\ &= -\left(\gamma \left(\frac{\bar{T}_s - t}{\bar{T}_s}\right)^{2h+3-\ell} + \frac{(2+2h)(\bar{T}_s - t)^{2h+2-\ell}}{\bar{T}_s^{2h+3-\ell}}\right) \\ &\quad (e^{-\gamma t} e_i(0) + c_i) \end{aligned} \quad (87)$$

As $h > \frac{\mathcal{D}(G)}{2}$ and $\ell \leq \mathcal{D}(G) - 1$, there holds $\lim_{t \rightarrow \bar{T}_s^-} \dot{e}_i(t) \geq 0$.

To derive the lower bound of the left-hand limit of $\dot{e}_i(t)$ at \bar{T}_s , note that (86) implies $e_i(t) \geq \frac{1}{\rho^2(t)} e^{-\lambda t} e_i(0)$ by Lemma 6, together with (25), there holds

$$\begin{aligned} \dot{e}_i(t) &= -\bar{\eta}(t)(x_i(t) - \min_{j \in \mathcal{N}(i)} \{x_j(t) + w_{ij}\}) \\ &\leq -\bar{\eta}(t)(x_i(t) - (x_j(t) + w_{ij})) \end{aligned} \quad (88)$$

$$= -\bar{\eta}(t)(e_i(t) - e_j(t)) \quad (89)$$

$$\leq -\bar{\eta}(t) \left(\frac{e^{-\lambda t} e_i(0)}{\rho^2(t)} + \frac{(\bar{T}_s - t)^{2h+4-\ell}}{\bar{T}_s^{2h+4-\ell}} (e^{-\gamma t} e_j(0) + c_j) \right) \quad (90)$$

where in (88) we assume $j \in \mathcal{F}_{\ell-1}$ is true parent node of i , and (89) uses (1), and (90) uses Lemma 9. Then it follows from (26) and (87) that $\lim_{t \rightarrow \bar{T}_s^-} \dot{e}_i(t) \leq 0$. Therefore, our result holds by Squeeze theorem [32].

Proof of the claim in Remark 7: It follows from (44) that

$$\begin{aligned} \dot{x}_i(t) &= -\eta(x_i(t) - \min_{j \in \mathcal{N}(i)} \{|x_j(t)| + w_{ij}(t)\}) \\ &\geq -\eta(x_i(t) - w_{\min}), \forall i \in V \setminus S, \end{aligned} \quad (91)$$

where (91) uses (36). By comparison principle, we obtain

$$x_i(t) \geq e^{-\eta t} (x_i(0) - w_{\min}) + w_{\min}, \quad (92)$$

leading to $x_i(t) > 0$ for $t \geq 0$ if $x_i(0) \geq 0$, or $x_i(t) \geq 0$ for $t \geq \frac{1}{\eta} \ln \frac{w_{\min} - x_i(0)}{w_{\min}}$ otherwise.

Proof of Lemma 11: The proof for (46) is trivial. For $i \notin S$, we consider three cases: 1) $e_i(t) > 0$; 2) $e_i(t) < 0$; and 3) $e_i(t) = 0$. In the first case, let j be the true parent node of node i , it follows from (35) that

$$\begin{aligned} \dot{V}_i(e_i(t)) &= \dot{e}_i(t) = -\eta(x_i(t) - \min_{j \in \mathcal{N}(i)} \{x_j(t) + w_{ij}(t)\}) \\ &\leq -\eta(x_i(t) - (x_j(t) + w_{ij} + u_{ij}(t))) \end{aligned} \quad (93)$$

$$= -\eta(x_i^* + w_{ij} + e_i(t) - (x_j^* + e_j(t) + w_{ij} + u_{ij}(t))) \quad (94)$$

$$= -\eta e_i(t) + \eta e_j(t) + \eta u_{ij}(t)$$

$$\leq -\eta V_i(e_i(t)) + \eta V_j(e_j(t)) + \eta |u(t)| \quad (95)$$

where (93) uses (37), (94) uses (1) and (9), and (95) uses the

fact that $e_i(t) > 0$ and $V_i(e_i(t)) = e_i(t)$.

In the second case, let j be the current parent node of node i , i.e., $j \in \mathcal{P}_i(t)$, it follows from (35) that

$$\begin{aligned} \dot{V}_i(e_i(t)) &= -\dot{e}_i(t) = \eta(x_i(t) - \min_{j \in \mathcal{N}(i)} \{x_j(t) + w_{ij}(t)\}) \\ &= \eta(x_i^* + e_i(t) - (x_j^* + e_j(t) + w_{ij} + u_{ij}(t))) \end{aligned} \quad (96)$$

We need to consider two subcases. Firstly, suppose j in (96) is also a true parent node of node i . By (1), (96) reduces to

$$\begin{aligned} \dot{V}_i(e_i(t)) &= \eta(e_i(t) - e_j(t) - u_{ij}(t)) \\ &\leq -\eta V(e_i(t)) + \eta V(e_j(t)) + \eta |u(t)| \end{aligned} \quad (97)$$

where (97) uses the fact that $e_i(t) < 0$ and $V_i(e_i(t)) = -e_i(t)$.

Suppose in (96) $j \notin \mathcal{P}(i)$. By (45), (96) reduces to

$$\begin{aligned} \dot{V}_i(e_i(t)) &\leq \eta(\zeta(x_j^* + w_{ij}) + e_i(t) - (x_j^* + e_j(t) + w_{ij} + u_{ij}(t))) \\ &\leq \eta(\zeta(x_j^* + w_{ij}) + e_i(t) - \zeta(x_j^* + e_j(t) + w_{ij}) - u_{ij}(t)) \end{aligned} \quad (98)$$

$$\leq -\eta V_i(e_i(t)) + \eta \zeta V_j(e_j(t)) + \eta |u(t)| \quad (99)$$

where (98) uses the fact that $x_j(t) = x_j^* + e_j(t) \geq 0$ and $w_{ij} > 0$, and (99) uses that $V_i(e_i(t)) = -e_i(t)$ as $e_i(t) < 0$.

For the case $e_i(t) = 0$. If the condition in (47) holds, then $|u(t)| = e_j(t) = 0$ for all $j \in \{1, \dots, n\}$. From (35),

$$\begin{aligned} \dot{V}_i(e_i(t)) &= \bar{\xi} \dot{e}_i(t) = -\bar{\xi} \eta(x_i(t) - \min_{j \in \mathcal{N}(i)} \{x_j(t) + w_{ij}(t)\}) \quad (100) \\ &= -\bar{\xi} \eta(x_i^* - \min_{j \in \mathcal{N}(i)} \{x_j^* + w_{ij}\}) = 0 \end{aligned} \quad (101)$$

where $\bar{\xi}$ in (100) obeys $\bar{\xi} \in [-1, 1]$ by (43), and (101) uses (1). Combining (95), (97), (99) and (101), (47) holds.

Proof of Lemma 12: If $1 < \eta < (1/\zeta)^{\frac{1}{\mathcal{D}(G)}}$, there exists $d > 1$ such that $d\eta\zeta < 1$. Consequently, there exists $d > 1$ such that $d\bar{\lambda}_{ii} < 1$ for all $i \in \{1, \dots, n\}$, where $\bar{\lambda}_{ii} = \zeta\eta$ by (48), given that $i \notin \mathcal{P}(i)$. From (48), $d\bar{\lambda}_{ij} > 1$ can only happen when $i \notin S$ and $j \in \mathcal{P}(i)$, as in this case $\bar{\lambda}_{ij} = \eta > 1$. Therefore, the maximum value induced by such cyclic compositions arises from node sequences: i_1, i_2, \dots, i_r , where i_ℓ is a true parent node of node $i_{\ell-1}$ for $\ell \in \{2, \dots, r\}$. Now we consider two cases: 1) $i_r \in S$; and 2) $i_r \notin S$. In the former case, it follows from Definition 2 that $r \leq \mathcal{D}(G)$, together with (48), we obtain

$$d\bar{\lambda}_{i_1 i_2} \times d\bar{\lambda}_{i_2 i_3} \times \dots \times d\bar{\lambda}_{i_r i_1} = d^r \frac{0.5\eta^{r-1}}{\eta^{\mathcal{D}(G)-1}} \leq 0.5 \cdot d^{\mathcal{D}(G)},$$

implying the existence of $d_1 > 1$ such that $0.5 \cdot d_1^{\mathcal{D}(G)} < 1$.

In the latter case, there holds $r \leq \mathcal{D}(G) - 1$, and $i_1 \notin \mathcal{P}(i_r)$ by Lemma 1 in [12], as otherwise $\mathcal{D}(G)$ would become infinite. By (48), we have

$$\begin{aligned} d\bar{\lambda}_{i_1 i_2} \times \dots \times d\bar{\lambda}_{i_{r-1} i_r} \times d\bar{\lambda}_{i_r i_1} &\leq d^r \eta^r \zeta \\ &< d^{\mathcal{D}(G)-1} (1/\zeta)^{\frac{\mathcal{D}(G)-1}{\mathcal{D}(G)}} \zeta = d^{\mathcal{D}(G)-1} \zeta^{\frac{1}{\mathcal{D}(G)}}. \end{aligned}$$

As $\zeta < 1$ by (45), there must exist $d_2 > 1$ such that $d_2^{\mathcal{D}(G)-1} \zeta^{\frac{1}{\mathcal{D}(G)}} < 1$. Let $d = \min\{d_1, d_2\}$ be the diagonal operator factor of D , our claim follows.